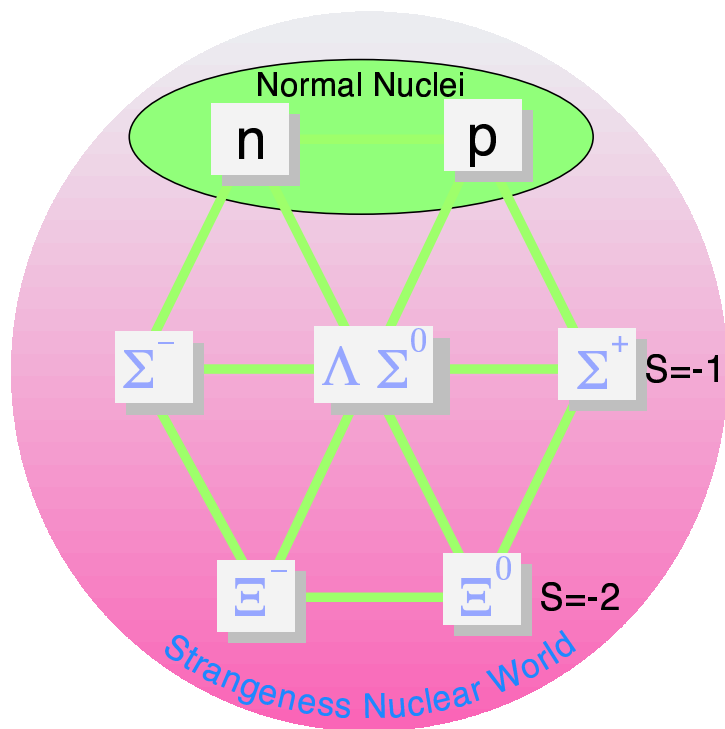Letter of Intent
for
New Generation Spectroscopy
of
Hadron Many-Body Systems
with Strangeness $S = -2$ and -1

December 31, 2002

J-PARC Strangeness Nuclear Physics Group

K. Imai(Contact Person), M. Nakamura, H. Funahashi, M. Yosoi
Kyoto University
T. Nagae, M. Ieiri, H. Noumi, H. Outa, M. Sekimoto, H. Takahashi, Y. Sato, A. Toyoda
KEK
T. Fukuda, P.K. Saha
Osaka Electro-Communication University
K. Nakazawa
Gifu University
K. Yamamoto, T. Yoshida
Osaka City University
O. Hashimoto, K. Maeda, H. Tamura, S.N. Nakamura, T. Takahashi, Y. Fujii, H. Kanda
Tohoku University
T. Kishimoto, A. Sakaguchi, S. Ajimura, Y. Shimizu, S. Minami, T. Itahashi, T. Hayakawa
Osaka University
M. Iwasaki, K. Itahashi, K. Tanida, Y. Matsuda
RIKEN
J.S. Song, I.G. Park, C.S. Yoon, S.H. Kim
Gyeongsang National University, Korea
J.Y. Kim
Chonnan National University, Korea
M.Y. Pac
Dongshin University, Korea
J.K. Ahn, I.K. Yoo
Pusan National University, Korea
H. Bhang, M. Youn
Seoul National University, Korea
S. Zhou, L. Zhu
China Institute of Atomic Energy, China
B. Bassalleck
University of New Mexico, USA
L. Tang
Hampton University, USA
P. Markowitz, B. Raue, J. Reinhold
Florida International University, USA
M. May, R.E. Chrien, A. Rusek, P.H. Pile
Brookhaven National Laboratory, USA
S. Choi
Temple University, USA
Ed. Hungerford
University of Houston, USA
G. Franklin, R. Schumacher, B. Quinn
Carnegie Mellon University, USA

T.R. Saitoh, A. Banu

GSI, Germany

J. Arvieux

Institut de Physique Nucleaire d'Orsay, France

P. Kienle, M. Cargnelli, J. Marton, J. Zmeskal

Institute for Medium Energy Physics, Austria

S. Marcello, T. Bressani

Università di Torino, Italy

M. Agnello

Politecnico di Torino, Italy

A. Feliciello

INFN Sezione di Torino, Italy

P. Tlusty

Nuclear Physics Institute, Czech republic

Contents

1 Facility proposal for Strangeness Nuclear Physics

1.1 Introduction

The world of hadron and nuclei can be expanded by adding strangeness quantum number (S). Discovery of a new type or new state of nuclei has often provided us new physics. The strangeness nuclear physics is a frontier of nuclear physics with a good chance of such discovery. High intensity and high quality kaon and pion beams at 50-GeV proton synchrotron (PS) will certainly provide us such opportunities.

Strangeness nuclear physics has attracted much attention for various reasons. First of all, a hyperon can penetrate deep inside a nucleus due to the lack of Pauli exclusion. Recent spectroscopy of heavy hypernuclei clearly demonstrated the s-shell structure in nuclei as heavy as Pb, which has only been seen by a probe such as a hyperon. Recently it was experimentally verified that an addition of a Λ hyperon shrinks the size of the ^{6}Li core nucleus. Even a single hyperon can change the properties of nuclei which provide a new playground for nuclear physics. Some nuclei become bound by a Λ and then one can study their electro-magnetic properties by γ transitions, otherwise not possible.

One can also study the properties of hyperons in nuclear matter by studying hypernuclei. Hadrons in nuclei have been a big topics in nuclear and hadronic physics recently. Hypernuclei are unique in this context. Since a hyperon such as the Λ is stable in nuclei, one can study not only the energy of various states but also the lifetime, magnetic moment, etc. The hypernuclei give a unique place to study the nucleon-hyperon weak interaction. One of the motives for studying the non-mesonic weak decay of hypernuclei is to investigate the origin of the $\Delta I = 1/2$ rule in the hyperon decays.

Since the QCD was established, models such as the quark-cluster model were proposed to describe the nuclear force based on QCD and quark structure of the nucleon. The flavor SU(3) symmetry is well established in meson and baryon spectroscopy. It is natural to extend such studies in the frame of SU(3) to refine and verify these models. The experimental studies of hyperon-nucleon and hyperon-hyperon interaction, therefore become important. We can learn about the hyperon-nucleon interaction by the scattering experiments, though very difficult, and also by the study of hypernuclei. The recent observations of "fine structure" of hypernuclei with the Hyperball have clarified the $\Lambda - N$ spin-spin and spin-orbit interactions. The binding energy of a double Λ hypernucleus is a unique source of information on the $\Lambda - \Lambda$ interaction.

It should be noted that the hyperon-nucleon interaction is essential to understand the structure of hypernuclei. It is also important for the astrophysics of neutron stars, since there can be a considerable amount of hyperons in the core of neutron stars depending on the interactions.

After QCD was accepted, the quark degree of freedom in a nucleus has been a major topic in nuclear physics. It was speculated that the partial deconfinement of quarks in nuclear matter may be seen in hypernuclei. So far there has been no such evidence in the case of Λ hypernuclei. However, in the case of $S=-2$, the 6-quark H-dibaryon has not been ruled out yet, and there is still the possibility of H-nuclei being the ground state of $S=-2$ nuclei. One can not deny the possibility that the strange quark matter is a QCD ground state rather

than nuclei. The $S=-2$ nuclei are the first step toward multi-strangeness systems. The experimental studies of $S=-2$ nuclei are, therefore, extremely important in relation to this question.

1.2   Recent progress in Strangeness Nuclear Physics

Since the discovery of a hyperfragment in nuclear emulsion in 1953, the strangeness nuclear physics has a long history.

However, the recent progress (within a decade) is rather outstanding, motivated by the physics described in the introduction. The followings are some examples;

1) High resolution (π^+, K^+) spectroscopy at SKS showed fine structure such as core excited states by achieving 1.5 MeV resolution (Fig. 1 left).

2) Lifetime of hypernuclei was measured up to Y and is already saturated at C-nuclei. The branching ratio of the weak decay was also measured up to Y. Observed n/p ratio can not be explained by current theories.

3) Bound Σ hypernuclei were established in the case of $^4_\Sigma$He.

4) The cross sections of Σ^+-p elastic scattering were measured in the region of 400-700 MeV/c with a scintillating fiber detector.

5) The existence of double-Λ hypernuclei was established by their cascade weak decays, and the binding energy of $^6_{\Lambda\Lambda}$He was measured for the first time without ambiguities(Fig. 1 right).

6) The γ spectroscopy of hypernuclei became possible in a few-keV resolution with the Hyperball. The fine structures due to the spin-spin and spin-orbit interaction were observed(Fig. 2).

7) The first evidence of Ξ-nucleus was observed.

Some interesting experiments are still on-going, in analyses, or in preparation to run in a year or so. Even before the 50-GeV PS operation, we may have a chance to find new interesting results.

1.3   Initial program of Strangeness Nuclear Physics

High-intensity kaon beams which will be available at the 50-GeV PS are quite unique in the world. In particular, the K^- beam at 1.8 GeV/c is a very efficient tool to implant $S=-2$ into normal nuclei through an abundant production of Ξ^-'s. Spectroscopic studies of $S=-2$ many-body systems will be carried out for the first time.

Various kinds of interesting experiments in this field have been already discussed in several international workshops. Here, we have selected several experiments which have physics importance, urgency, and technical feasibility at present.

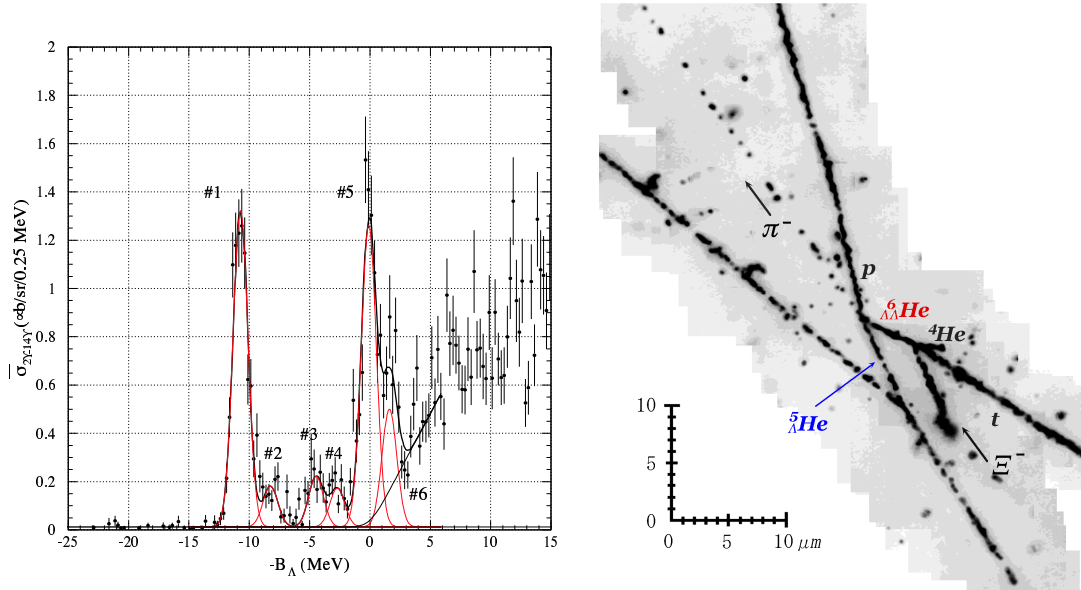a) Spectroscopy of Ξ-hypernuclei with the (K^-, K^+) reaction.

Figure 1: Left: The $^{12}_{\Lambda}$C spectrum measured with the (π^+,K^+) reaction by using the SKS spectrometer in KEK-PS E369.

Right: A $^{6}_{\Lambda\Lambda}$He nucleus was emitted from the point of Ξ^- hyperon capture at rest. The nucleus decayed to p, π^- and $^{5}_{\Lambda}$He nucleus, and $^{5}_{\Lambda}$He also decayed to two single charged particles and neutral one. $\Lambda\Lambda$interaction energy was uniquely measured as weak attractive interaction with $1.01 \pm 0.20 \,^{+0.18}_{-0.11}$ MeV.

b) Spectroscopy of double-Λ hypernuclei with sequential pionic decays and the (K^-,K^+) reaction.

c) Hypernuclear γ-ray spectroscopy of various hypernuclei with the upgraded Hyperball.

d) High-resolution (200 keV) spectroscopy of hypernuclei with the $(\pi^{\pm},K^+)$ reactions.

e) Hyperon-proton scattering experiments measuring the cross sections of $\Xi^-p \to \Xi^-p$ and $\Xi p \to \Lambda\Lambda$ reactions and polarization variables in Λ-p and Σ^+-p elastic scattering.

f) Search for deeply-bound Kaonic states.

The subjects listed above cover a very wide range of physics. However, the requests for the beams are mainly focused on two beam lines: K1.8 and K1.1 (the numbers are the maximum beam momentum.) Both beam lines should have the K^- beam intensity of $\sim 10^7$/sec. with a good K/π ratio of ≥ 1 at the maximum beam momentum. The former beam line, K1.8, is used for the experiments on $S=-2$ with K^-: subjects a), b), e), and possibly f). The latter one, K1.1, is for the experiments on $S=-1$ with K^- and $\pi^{\pm}$: subjects c), d), e), and f).

Here, we propose two experiments, subjects a) and c), as our immediate goals when new beams at the 50-GeV PS will be available at the designed K^- beam intensity of 10^7/sec. at K1.8 and K1.1, respectively. As for the detector systems, we will utilize the existing ones: the SKS spectrometer for Ξ^- hypernuclei spectroscopy with the (K^-,K^+) reaction, and
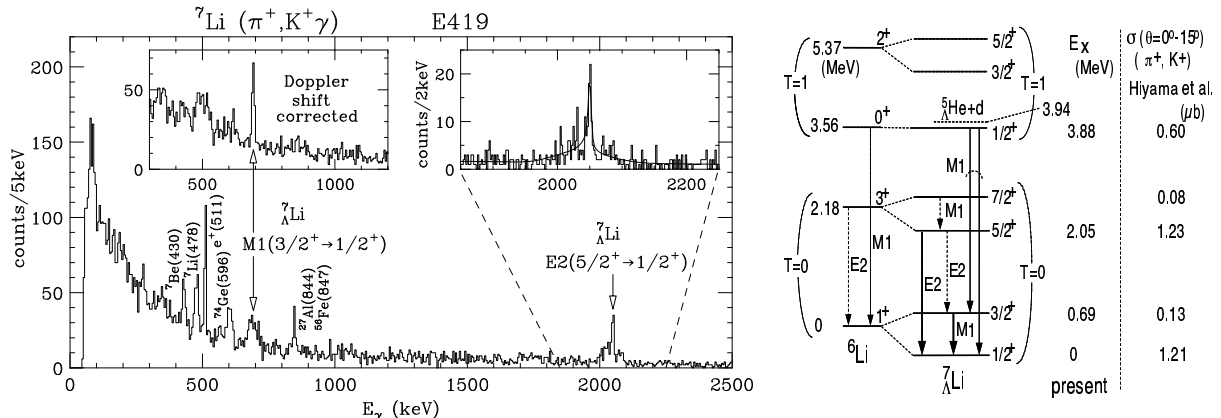
Figure 2: γ-ray spectrum of $^{7}_{\Lambda}$Li measured with Hyperball (KEK E419)(left) and the level scheme obtained from this experiment (right). We observed $M1(\frac{3}{2}^{+}\rightarrow\frac{1}{2}^{+})$ and $E2(\frac{5}{2}^{+}\rightarrow\frac{1}{2}^{+})$ transitions of $^{7}_{\Lambda}$Li at 692 keV and 2050 keV, respectively, and two M1 transitions from $\frac{1}{2}^{+}$,T=1 state to the ground state doublet.

the Hyperball detector system for hypernuclear γ-ray spectroscopy. Both detector systems should be upgraded for the new experiments, which will be described in the later sections.

When the K^{-} beam intensity would be low, $10^{5} \sim 10^{6}$/sec., in the commissioning stage of the 50-GeV PS, we could start from hypernuclear γ-ray spectroscopy in singles measurement which does not require the designed beam intensity. At the K^{-} beam intensity of $\sim 10^{6}$/sec., the Ξ^{-}-hypernuclei spectroscopy with the (K^{-},K^{+}) reaction could be carried out from light to medium-heavy target nuclei where the production yields are larger than those for heavy nuclei such as ^{208}Pb. Also, a new hybrid-emulsion measurement with the beam intensity of 10^{5} K^{-}'s/sec. and a good K^{-}/π^{-} ratio of ~ 10 would be an option at K1.8. The measurement aims for observing ~ 100 double-Λ hyperfragments in this beam condition. Of course, as the K^{-} beam intensity increases, we could proceed the Ξ^{-}-hypernuclei spectroscopy for heavier targets to determine the Ξ^{-}-nucleus potential parameters in nuclear matter by extrapolation. Also, the $\gamma-\gamma$ coincidence measurements will be easily carried out in hypernuclear γ-ray spectroscopy in a wide mass-number range.

In this stage, our minimum requirement for the beam line configuration is that the experimental areas at K1.8 and K1.1 should be prepared separately, so that we could minimize the time loss for switching the beams between two lines. The proposed idea is to have the K1.1 as a branch from K1.8 with a beam switching magnet just after the first mass-separator stage. Thus, at least, we can prepare two experimental setups at K1.8 and K1.1 at the same time. Then, we can deliver the beam for one of them. Of course, we hope to have two beam lines to be operated at the same time in the earliest possible stage.

Once these beam lines and detector systems are established in the new experimental hall, we will extend our studies for other subjects b), d), e) and f) after reaching our immediate goals. We could proceed them with minor investments for each experiment.

4

1.4 Kaon beam lines for Strangeness Nuclear Physics

K1.8 beam line

Design work of the K1.8 beam line is in progress, as shown in Fig. 3. This beam line has two stages of electrostatic separators (ES) with two mass slits (MS1 and MS2) in order to separate kaons from pions and others at the level of the K/π ratio greater than 1. A beam spectrometer system is located after MS2, which comprises QQDQQ magnets. This spectrometer system is designed to achieve a momentum resolution of as good as 2.4×10^{-4} (in σ) when a position resolution of 200 μm is realized in tracking chambers placed before and after the QQDQQ magnets. Secondhand magnets and ESs will be used for K1.8, except for a few of the front-end elements, to save the construction cost. Particularly, the last bending magnet (D4) is donated from Saclay/Saturne, which was used as a beam analyzer.

The beam envelope of the K1.8 beam line is calculated by TRANSPORT, as shown in Fig. 4. Design parameters of the K1.8 beam line is listed in Table 1.

One can branch another beam line at the D3 magnet. Connecting the QDQ magnets after D3, a beam line with shorter length can be constructed. An intense kaon beam at around or lower than 1 GeV/c can be utilized although the kaon purity has to be sacrificed to some extent. This branch line will be useful and effective to run an experiment when the K1.8 experiment is at a preparation stage, and *vice versa*.
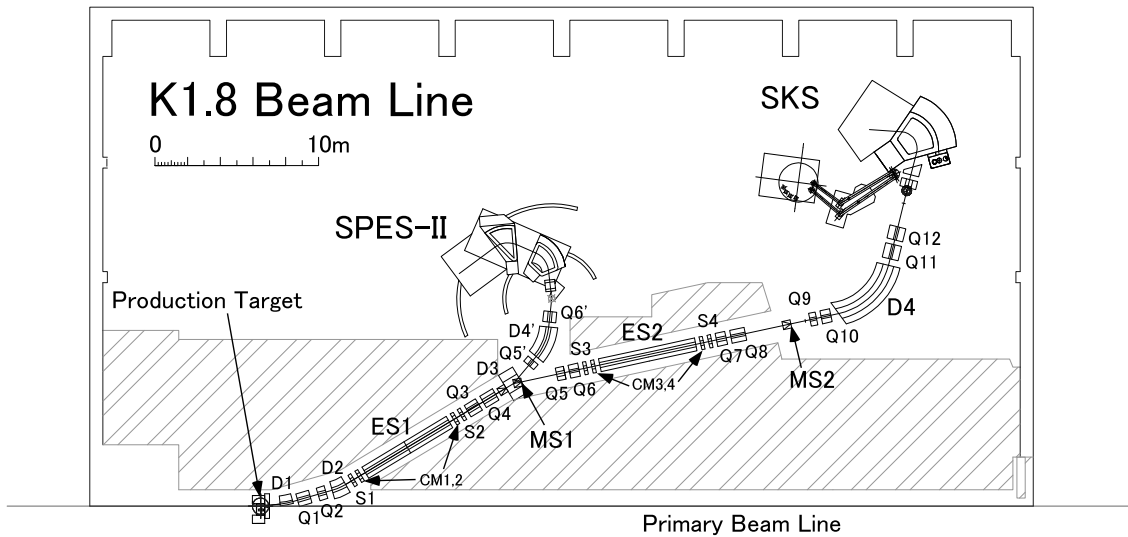
Figure 3: Plan view of the K1.8 beam line.

K1.1 beam line

A separate design of the low energy separated kaon beam line for strangeness nuclear physics, K1.1, is also under way. A current design of K1.1 is shown in Fig. 5. This beam line has two cross field type electrostatic separators to maintain the purify of K^- at the level of $K^-/\pi^- \sim 1$ below 1.1 GeV/c. The beam line length and acceptance are estimated to be as
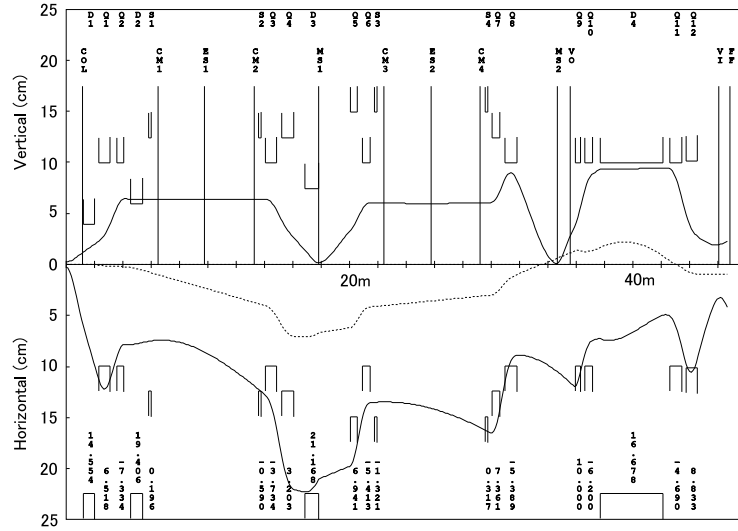
Figure 4: Beam envelope of the K1.8 beam line calculated by TRANSPORT.

Table 1: Design parameters of the K1.8 and K1.1 beam lines.

	K1.8	K1.1
Acceptance (msr·%)[1]	7.5	16.5
Length (m)	46.8	24
K$^-$ flux (/sec)[2]	4.7×10^6	6×10^6
purity (K$^-$/π^-)[3]	>2	>2

[1] The acceptance is evaluated by TURTLE.
[2] Kaon production cross section is estimated by the Sanford-Wang formula, assuming the 50-GeV proton beam of 15μA on the Ni target of 5.4 cm long.
[3] So-called cloud pions are not taken into account.

short as 24 m and as large as 16.5 mr·%. The kaon intensity is expected to be upto a several MHz at 1.1 GeV/c. Design parameters of the K1.1 beam line is listed in Table 1.

K1.1 Beam Line
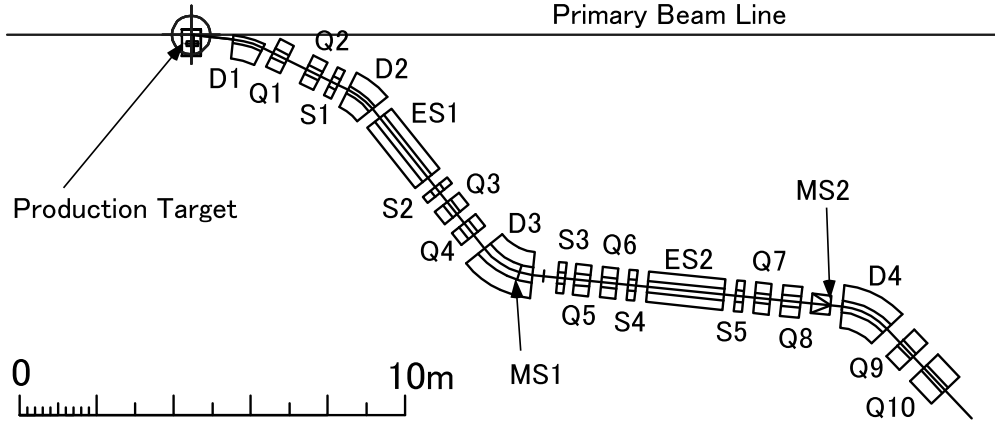
Figure 5: Plan view of the K1.1 beam line.
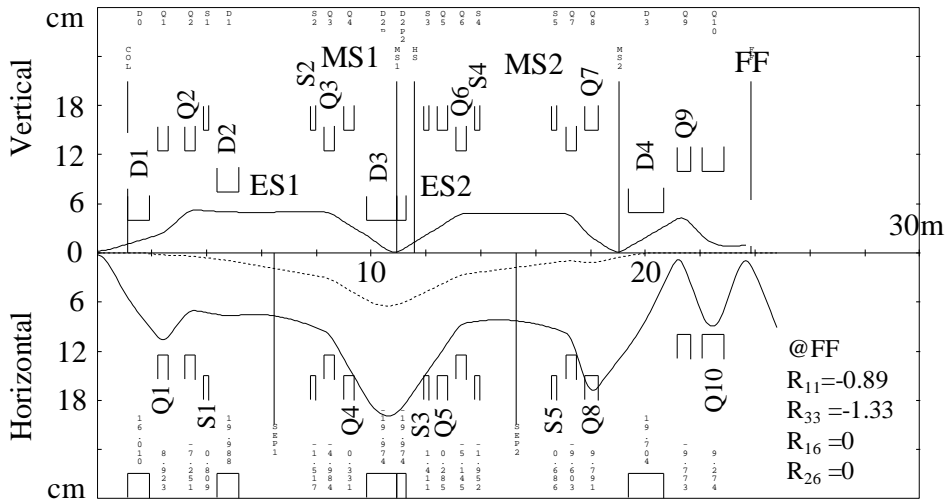
Figure 6: Beam envelope of the K1.1 beam line calculated by TRANSPORT.

1.5 International Collaborations

Since 1980's, BNL-AGS and KEK 12-GeV PS have been the two major facilities in the world for Strangeness Nuclear Physics after the shutdown of CERN PS for K^- beams. The international collaboration between US and Japan by using these two accelerators has been one of the most successful ones in this field.

BNL-AGS took full advantage of higher K^- beam intensities which were essential for Σ hypernuclei, H-dibaryon search, double-Λ hypernuclei, etc. However, the allocated beam times for Strangeness Nuclear Physics experiments in total were not so enough to conduct all the possible experiments. In contrast, new detector systems based on new ideas and

techniques were developed at KEK-PS to overcome the lower beam intensities: the SKS spectrometer for the (π^+,K^+) reaction, the Hyperball detector for hypernuclear γ-ray spectroscopy, hybrid-emulsion measurements for double-Λ hypernuclei, scintillating fiber (SCIFI) detectors and a bulk scintillator imaging detector for hyperon scattering measurements, etc. Also, the physics programs have been carefully selected one another to make them complimentary.

Some of the highlights are the collaborations in a series of experiments (E774, E887, E905) on Σ hypernuclei, H-dibaryon and double-Λ hypernuclei search experiments (E813, E836, E885, E906), hypernuclear γ-ray experiments (E929, E930), and so on. In the recent several experiments (E906, E929, E930), Japanese participants took a major role bringing new detectors constructed in Japan.

At the 50-GeV PS, the US physicists in this field are interested in contributing to Japan in return. Moving some beam line elements such as magnets, electro-static separators, power supplies, from the AGS D6 beam line has been discussed seriously. Also, there is an idea to construct a K^+ spectrometer for the (K^-,K^+) reaction by utilizing an existing spectrometer magnet, MRS.

Korean physicists have been working at KEK PS in several experiments with the SKS spectrometer, hybrid-emulsion, SCIFI detectors for more than 10 years. Some graduate students have already written up their Master and Doctor theses from these experiments. They eagerly want to extend this activity at the 50-GeV PS.

New international collaborations are now in progress at JLab and DAΦNE. Their experiments will be mostly on spectroscopy of $S=-1$ (Λ and Σ) hypernuclei in the different reactions of (e,e'K^+) and $(K^-_{Stopped},\pi^{\mp})$, in which the states to be excited would be complimentary with each other. They are interested in comparing their data with the results from the Hyperball in the (K^-, π^-) reaction. Also, they would like to extend their studies into the $S=-2$ systems at the 50-GeV PS.

1.6 Summary

We propose to construct two secondary K^- beam lines, K1.8 and K1.1, to carry out new generation hypernuclear spectroscopy with $S=-2$ and $S=-1$, respectively. We will utilize the existing two detector systems, the SKS spectrometer and Hyperball detector, with some upgrades.

Our immediate goals are the Ξ^- hypernuclei spectroscopy with the (K^-,K^+) reaction and the next-stage hypernuclear γ-ray spectroscopy in a wide variety of targets. The former experiment will give us an entrance to the quite new hadron many-body systems with $S=-2$ for the first time. It will be a great step into multi-strangeness world to reveal the role of strangeness in high-density nuclear matter. The latter experiment will fully investigate the world of Λ hypernuclei in wide ranges of mass number and Z/N (isospin) in high precision. It may give rise to new surprises and new phenomena on deeply-bound many-body systems.

There also exists many other interesting experiments in Strangeness Nuclear Physics waiting for the new beams. We strongly hope that the secondary beam lines would be properly equipped in the new experimental hall, so that we could carry out these important experiments in time.

2 Proposal for Spectroscopic Study of $S = -2$ Systems

The high intensity K^- beam at $\sim$1.8 GeV/c available at the 50-GeV PS is quite unique to open a new frontier of strangeness nuclear physics in the spectroscopic studies of strangeness $S=-2$ systems; here, the $S=-2$ systems include Ξ-hypernuclei, double-Λ hypernuclei, and possibly H-hypernuclei. This is not only a step forward from the $S=-1$ systems as a natural extension, but also a significant step to explore the multi-strangeness hadronic systems; in the course of the limit, strange hadronic matter (S=-∞) in the core of a neutron star is our concern. Also, it is important to extract some information on ΞN and Λ-Λ interactions from the spectroscopic data, considering the fact that there exist almost no experimental data on these interactions at this moment. Hence, we can explore the SU(3) character of the strong forces of QCD.

The (K^-,K^+) reaction is one of the best tools to implant the $S=-2$ through an elementary process K^-+p $\rightarrow$ K^++Ξ^-, the cross section of which in the forward direction has a broad maximum around this energy as shown in Fig 7. The angular distribution is backward peak in the center-of-mass (c.m.) system. Since no meson of strangeness two is known to exist, there is no meson exchange (t-channel) contribution and a baryon exchange (u-channel) mechanism is dominant. However, owing to kinematics, the cross section is still peaked to forward angles in the lab. frame, which makes experimental detection efficient.
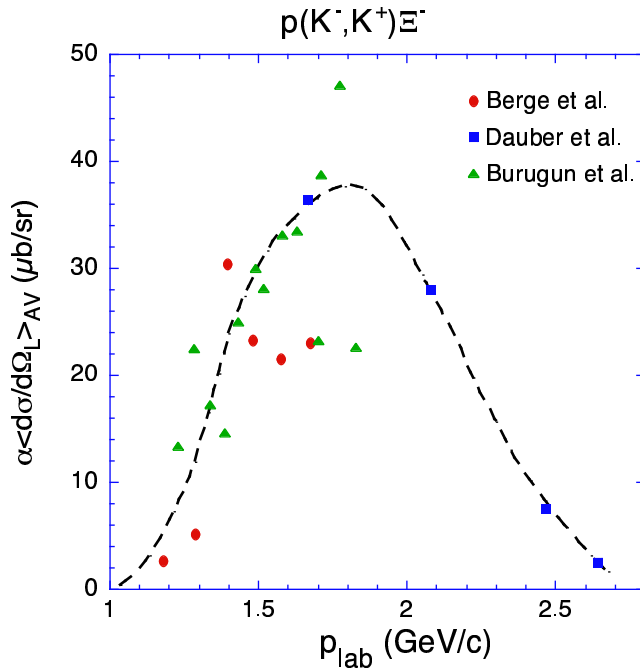

Figure 7: Incident momentum dependence of the production cross section of the K^-+p $\rightarrow K^+$+Ξ^- reaction.

At present, the experimental information on the $S=-2$ systems mainly comes from several emulsion data in limited statistics and with poor identifications.

9

As for the Ξ-hypernuclei, there exist some hints of emulsion events for the existence. However, it is still not conclusive. Some upper limits on the Ξ-nucleus potential have been obtained from the production rate in the bound region of a Ξ-hypernucleus via the (K^-,K^+) reaction.

So far, we had only three emulsion events to confirm the existence of double-Λ. However, one unique event cleanly identifying the $^6_{\Lambda\Lambda}$He has been found in a hybrid-emulsion experiment, KEK-PS E373, recently. The mass of the $^6_{\Lambda\Lambda}$He and the $\Lambda - \Lambda$ interaction energy $\Delta B_{\Lambda\Lambda}$ has been measured for the first time. It demonstrates the $\Lambda - \Lambda$ interaction is weakly attractive; weaker than that estimated before.

A lot of searches for H-dibaryon have been carried out from the late 1980s to 1990s. No evidence has been observed so far. The observation of weak decays from the double-Λ hypernuclei limits the allowed mass range of the H-dibaryon very close to $2\times m_\Lambda$. In this respect, it is important to observe the lightest double-Λ hypernucleus to set the most stringent limit. There are suggestions that the H-particle may exist as a resonance and/or the "H"-type configuration might be mixed in the $S{=}{-}2$ systems.

In Fig. 8, a typical energy spectrum and decay thresholds for Ξ- and double-Λ hyper-nuclear configurations are shown. The energy difference between the $(\Xi^- p)$ system and the $(\Lambda\Lambda)$ system is only 28.3 MeV in free space. Therefore, a relatively large configuration mixing between $\Xi^- + A$ and $\Lambda\Lambda + (A-1)$ states is suggested. It should be noted that a mixing of the Σ component in Λ-hypernuclei is suggested to be several %, in which the energy difference between two states is $\sim$75 MeV. This mixing would be quite significant in heavy targets, because the Ξ^--hypernuclear levels are deeply bound with the aid of the large Coulomb potential. It is very interesting to investigate whether the single-particle picture of Ξ^- is valid or not in such a system.

In this letter of intent, we propose three experimental methods to explore the $S{=}{-}2$ systems:

1. Spectroscopy of Ξ-hypernuclei with the (K^-,K^+) reaction,

2. Study of double-Λ hypernuclei by sequential pionic decay,

3. γ-ray Spectroscopy of double-Λ hypernuclei.

The first method investigates the entrance channel of the $S{=}{-}2$ world. Produced Ξ-hypernuclear states eventually decay into several forms of double-Λ systems through a strong conversion process of $\Xi^- p \rightarrow \Lambda\Lambda$. The identification of the double-Λ hyper-fragments could be done by the second method if the pionic decay branch emitting a characteristic energy pion is large. This is the case for light hyper-fragments. The binding energy of the ground state of such light double-Λ hypernuclei can be measured.

The study of excited levels of double-Λ hypernuclei could be carried out via the same method as the first one, in principle, although we need further studies on the production mechanism to obtain much reliable estimation on the production rate. The measurement of the γ-ray transition of double-Λ hypernuclei is another way to investigate the excited levels. However, the energy range to be explored would be limited, because the population of double-Λ hypernuclei from the Ξ-hypernuclear formation in the (K^-,K^+) reaction tends to lower the neutron emission threshold close to the ground state. The study of decay
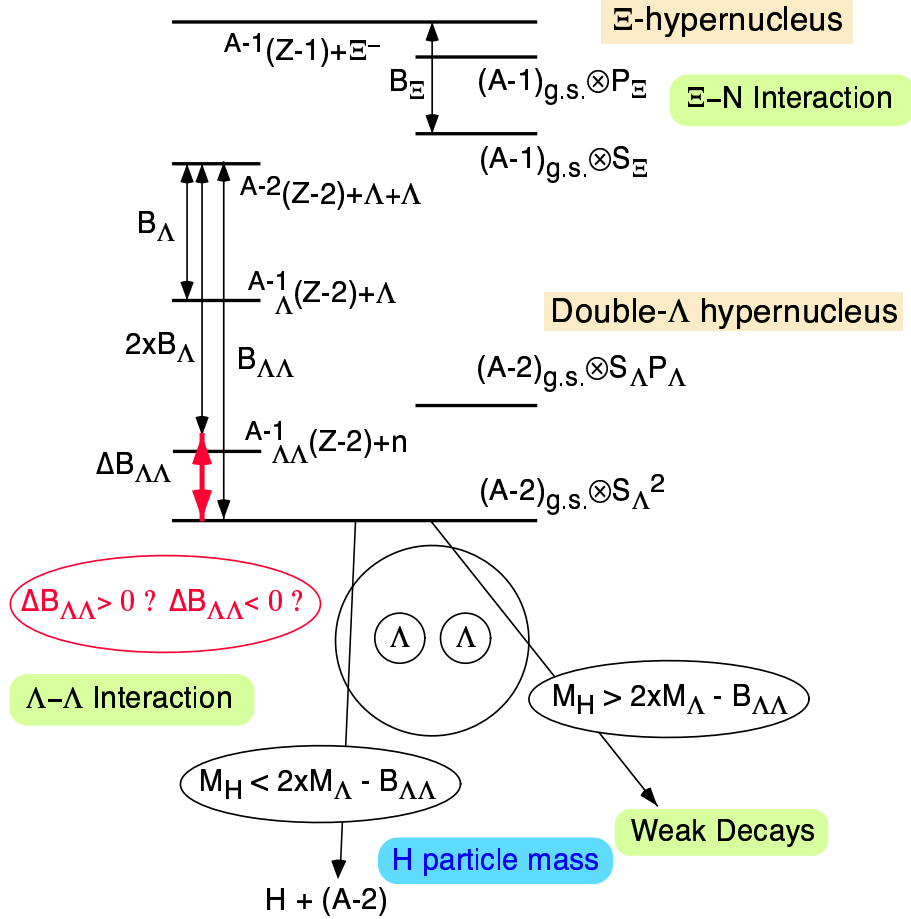
Figure 8: Typical energy spectrum and decay threshold for Ξ- and double-Λ hypernuclear configurations.

properties of double-Λ hypernuclei is another interesting subject to be investigated in the future: lifetime measurements of double-Λ hypernuclei, non-mesonic weak decay modes of double-Λ hypernuclei, etc.

2.1 Spectroscopy of Ξ Hypernuclei

2.1.1 Physics Interests

The Ξ-hypernuclei will play an essential role in our investigation of the $S=-2$ baryon-baryon interaction. Yet, at present, the existence of Ξ-hypernuclei cannot even be termed well established.

Unlike to Λ and double-Λ hypernuclear ground states which are long lived and decay via the weak interaction, Ξ-hypernuclei decay via the strong interaction through the $\Xi^-\mathrm{p}\rightarrow\Lambda\Lambda(Q = 28.3\mathrm{MeV})$ conversion. In this sense, the situation is very similar to Σ-hypernuclei in which the strong conversion process $\Sigma N \rightarrow \Lambda N(Q \sim 75\mathrm{MeV})$ exists and broaden the state. A naive semi-classical estimate of the spreading width for a Ξ^- single-particle state for an infinite nuclear matter gives us $\Gamma_\downarrow \sim 13$ MeV. However, for finite nuclei, the width would be reduced to be ≤ 1 MeV due to the reduction of phase space and overlap of wave functions, etc.

Therefore, it is expected that the spectroscopy of the Ξ-hypernuclei is promising. Here we use the (K^-,K^+) reaction in which we can use the same method for the (π^+,K^+) reaction in the Λ-hypernuclear spectroscopy. In fact, two reactions have a very similar characteristics of large recoil momentum of a produced hyperon: $p_{\Xi^-} \sim 500$ MeV/c and $p_\Lambda \sim 350$ MeV/c. Therefore, even for heavy targets well-separated peak structures are expected in spite of many possible excitations, because the spin-stretched configurations with $\ell_p + \ell_\Xi + J = even$ are strongly populated as in the case of the (π^+,K^+) reaction, or more strongly.

Convincing evidence for Ξ single-particle states would yield information on the Ξ single-particle potential and the effective ΞN interaction. It is predicted in a meson-exchange model that the Ξ well depth depends considerably on mass number, A. For example, the well depth in ^{207}Tl is estimated to be more than two times deeper than that in ^{11}B. This is because the space (Majonara) exchange is impossible within one-meson-exchange picture in the ΞN system, unlike the NN, ΛN, and ΣN systems. Hence, the p-wave attraction is expected to be strong in the ΞN, which leads to the substantial increase of ΞA attraction with A. This is an interesting prediction to be examined experimentally.

Knowledge of the depth of the Ξ-nucleus potential is important also for estimating the existence of strange hadronic matter with Ξ's. For a long time, it was believed that Σ^- hyperons would appear in neutron stars earlier (i.e., at lower densities) than even more light Λ hyperons due to their negative charge. However, recent data strongly suggest that the interaction of Σ^- with neutron-rich nuclear systems is strongly repulsive, which means Σ^- hyperons can no longer appear in neutron stars. It was argued that disappearance of Σ^- hyperons does not necessarily leads to crucial changes of neutron stars features if they were substituted effectively by Ξ^- hyperons. However, better understanding of Ξ^-N interaction is necessary for definite conclusions. With respect to the neutron star structure, it becomes much more important to investigate the Ξ dynamics than it was considered previously, because the Σ^--nuclear repulsion has been established.

For the experimental targets, we propose three targets, ^{28}Si, ^{58}Ni, and ^{208}Pb, to get the information of Ξ single-particle states in a wide mass-number range.

2.1.2 Experimental Apparatus

For the spectroscopy of the (K^-, K^+) reaction, we need two spectrometers like in the (π^+, K^+) reaction: a beam line spectrometer for the incident K^- and a K^+ spectrometer.

At this moment, we propose to construct a new beam line with a good K^-/π^- ratio of ≥ 1 and a good momentum resolution of $\sim 5 \times 10^{-4}$(FWHM). As for the K^-/π^- ratio, the 2-GeV/c beam line at BNL-AGS is an excellent example. This is essential to handle such a high intensity beam of 1×10^7/s. The momentum resolution in the beam line, however, is too poor to enable us to perform spectroscopic studies. The good momentum resolution better than 1×10^{-3} has been already achieved at the K6 beam line of the KEK 12-GeV PS. The last part of the beam line, after the mass separation, consists of a QQDQQ system to reconstruct the incident momentum. Thus, we need a combination of the two beam lines for the new K^- beam line.

K^- beam line

A 2-GeV/c kaon beam line for the JHF was designed by J. Doornbos [1]. In the design, he considered,

1) a good K/π separation,

2) a good resolution, and

3) a matching to a high-resolution pion line.

Referring to this design, H. Noumi designed the K1.8 beam line by mostly using the existing magnets at KEK. A schematic layout of the K1.8 beam line is shown in Fig. 9.

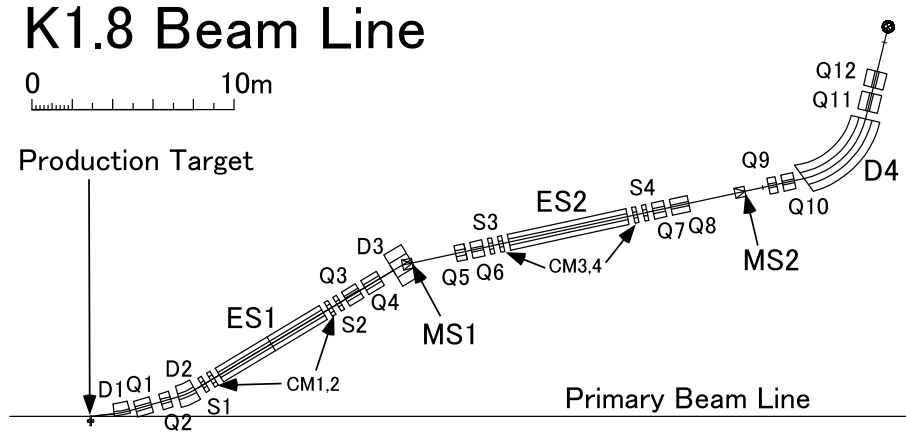Figure 9: Schematic layout of the K1.8 beam line.

As for the K/π separation, two-stage separator system is installed to attain K/π=2~5. The first stage acts like a preliminary clean up stage and defines a precise source for the second stage. In this way, the contamination due to cloud pions from neutral kaon decay near the production target and the contamination due to muons from pion decay in the channel

can be reduced one order of magnitude. Contamination from pions directly produced in the production target can be reduced by using multipoles to correct the aberrations which otherwise would cause long tails on the vertical pion distributions at the mass slits.

A beam line spectrometer is installed in the last part of the beam line. It consists of a QQDQQ system. Point to point focusing between the entrance and the exit of the QQDQQ system has the advantage that in the first order the momentum resolution becomes independent of multiple scattering. It is estimated that the momentum resolution of 5×10^{-4} could be achievable.

The first separation stage of the K1.8 beam line could be shared by another beam line. For that purpose, a bending magnet is installed just after the first mass slit.

In this design, the beam line has an angle and momentum acceptance of 7.5 msr·% and is 46.8 m long. Compared to the D-line at BNL-AGS, it is about 15 m longer because of the addition of the beam line spectrometer.

Table 2: Characteristics of the bending magnets

Bending Magnets	Field (kG)	Length (m)	Bending Radius(m)	Bending Angle(deg.)	Polegap (cm)
D1	13.099	0.8	4.584	10	8
D2	17.465	0.9	3.438	15	15
D3	19.051	1.018	3.152	18.5	15
D4	16.678	4.468	4.000	64	20

Table 3: Characteristics of the Quadrupole and Sextupole magnets

Quadrupole Magnets	Pole Field (kG)	Length (m)	Pole Radius(cm)
Q1	5.866	0.8	10
Q2	-6.601	0.5	10
Q3	-3.361	0.8	10
Q4	2.883	0.9	12.5
Q5	6.247	0.5	15
Q6	-4.872	0.6	10
Q7	6.625	0.6	12.5
Q8	-4.850	0.9	10
Q9	9.000	0.4	10.
Q10	-5.580	0.6	10
Q11	-4.221	0.9	10

Sextupole Magnets	Pole Field (kG)	Length (m)	Pole Radius(cm)
S1	0.1765	0.2	12.5
S2	-0.531	0.2	12.5
S3	-1.189	0.2	15.0
S4	-0.531	0.2	15,0

Separators:

The two separators are each 6 m long and have a vertical gap of 10 cm. The field over the gap is 750 kV. The useful horizontal aperture for the beam is 30 cm.

K^+ spectrometer

For the K^+ spectrometer, we will use the existing SKS spectrometer with some modifications. In the (K^-,K^+) reaction, the K^+ momentum corresponding to the production of Ξ-hypernuclei is around 1.2 GeV/c. In the (π^+,K^+) reaction, the SKS magnetic field is 2.2 T for 0.72 GeV/c. Therefore, the SKS maximum magnetic field of ~2.7 T does not allow us to put the central ray at 1.2 GeV/c. In Fig. 10, the setup of the SKS spectrometer for the (K^-,K^+) reaction is shown schematically.
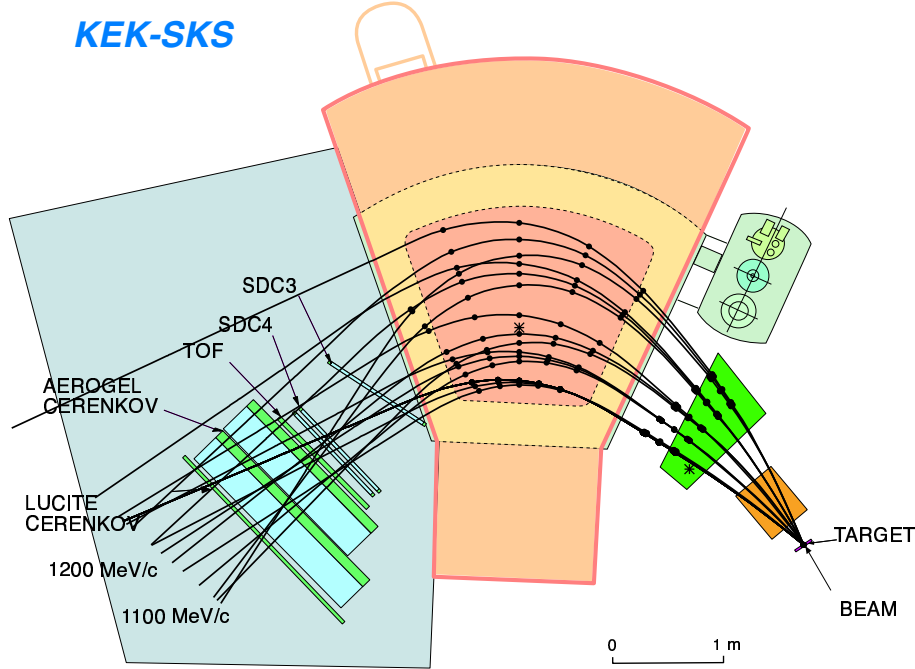
Figure 10: Schematic layout of the SKS spectrometer for the (K^-,K^+) reaction at 1.65 GeV/c.

Since the radius for the central momentum is larger than that for the (π^+,K^+) reaction, the target point is moved away from the magnet. So that, the acceptance of the spectrometer is reduced to be ~50 msr.

The optical property and the acceptance could be improved by installing a small dipole magnet and/or a quadrupole magnet at the entrance of the SKS magnet. The design study is still underway.

The energy resolution for the Ξ-hypernuclear spectroscopy in the (K^-,K^+) reaction is estimated as follows;

$$\Delta E^2 = \beta_{K^+}^2 \times \Delta p_{K^+}{}^2 + \beta_{K^-}^2 \times \Delta p_{K^-}{}^2 + \Delta E_{straggling}^2,$$

where Δp's are momentum errors of two spectrometers, and the last term comes from the energy loss straggling in a target. In contrast to the (π^+,K^+) reaction, the difference of the mean energy losses between incident and out-going particles is negligible. For a 2 g/cm^2 target, $\Delta E_{straggling} \sim$0.5 MeV. The Δp/p of the beam line spectrometer is designed to be 2×10^{-4}. Thus, the second term is (0.31 MeV)^2. The momentum resolution of the SKS is know to be expressed as,

$$\frac{\Delta p}{p} = (0.96 \pm 0.13) \times 10^{-4} p_K + (0.092 \pm 0.007)(\%).$$

Assuming that the first term mainly determined by the optical property is same and the second term by the multiple scattering is proportional to $1/p\beta$, Δp/p for p$_{K+}$=1.2 GeV/c is 0.17%. Therefore, the overall energy resolution would be $\Delta E = \sqrt{1.89^2 + 0.31^2 + 0.5^2}$= 2 MeV(FWHM).

2.1.3 Yield estimation

The production cross section of the Ξ-hypernuclei in the (K^-,K^+) reaction is calculated by Akaishi *et al.* [2] within the framework of the distorted-wave impulse approximation (DWIA) using the Green's function method. At present, we have very little information on the shape and the depth of Ξ^--nucleus potential. In the calculation, two types of the Ξ^--nucleus potential are used. One is Woods-Saxon type,

$$U_{\Xi^-}^{WS} = \frac{V_0 + iW_0}{1 + \exp\left\{(r-R)/a\right\}},$$

with V_0=-24 or 16 MeV, W_0=-1 MeV, R=1.1$\times$A$^{1/3}$ fm and a=0.65 fm. The other one is the folding-type potential. As the effective ΞN potential, Shinmura's potential [3] equivalent to the Nijmegen model-D interaction is used. The result is shown in Fig. 11. As seen from the figure, we can expect the cross section to be $\sim$0.1 μb/sr/MeV around the middle of the bound region for all types of potentials calculated.

Then, the expected yield for the ^{208}Pb target with 2-g/cm^2 thickness could be calculated as follows;

$$
\begin{aligned}
Y &= I_{Beam} \times 2g/cm^2/208g \times N_A \times \frac{d\sigma}{d\Omega} \times \Delta\Omega \times f_{decay} \times f_{eff} \\
&= 10^7 \times (2/208) \times 6.02 \times 10^{23} \times 0.1 \times 10^{-30} \times 0.05 \times 0.5 \times 0.5 \; events/sec \\
&\simeq 6 \; events/day,
\end{aligned}
$$

where $\Delta\Omega$ is the spectrometer acceptance, f_{decay} is the survival rate for K$^+$ decay-in-flight, and f_{eff} is the overall detector efficiency. So, even for the heaviest case, we could get enough statistics within $\sim$20 days to obtain spectroscopic information. Several peak positions for Ξ-orbitals with high angular momenta would be measured within the precision of $\leq$1 MeV, so that we can accurately determine the potential depth of the Ξ^--nucleus potential. For lighter targets such as ^{28}Si and ^{58}Ni, the yields are several times higher with the normalized target thickness of 2 g/cm^2.
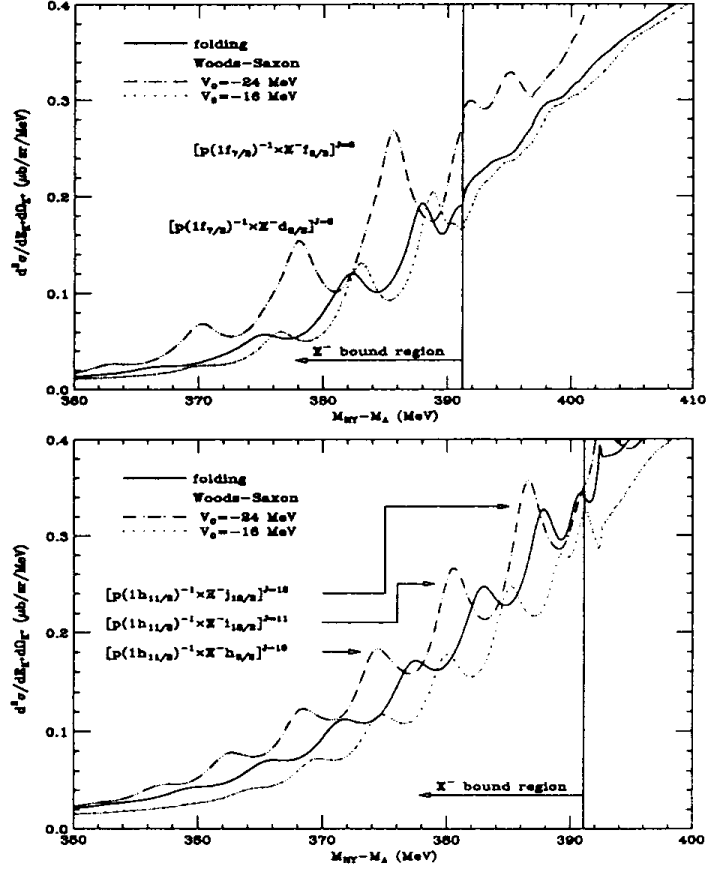
Figure 11: The Ξ^--hypernuclear spectra for the ^{58}Ni(K^-,K^+) and ^{208}Pb(K^-,K^+) reactions for p_{K^-}=1.65 GeV/c and θ_{K^+}=0° as a function of M_{HY}-M_A. The Ξ binding threshold is denoted by the vertical line. Spectrometer resolution is taken to be 2 MeV (FWHM).

Production of Double-Λ hypernuclei with the (K^-,K^+) reaction

Production of double-Λ hypernuclei is possible directly through a second order process; $K^-p \to (\pi,\rho,\omega)\Lambda, (\pi,\rho,\omega)p \to K^+\Lambda$ and $K^-p \to K^+\Xi^-$, $\Xi^-p \to \Lambda\Lambda$. However, a theoretical estimation [4] suggests the cross section to discrete double-Λ hypernuclear states would be rather small, of the order of a few nb/sr(Fig. 12). It is $\sim$1/100 of that for the Ξ-hypernuclear production. Thus, with a 2 g/cm^2 target of mass number $\sim$20, the production yield of $\sim$60 events/peak is expected for 100 days. This method has a unique advantage to allow us direct access to the spectroscopic information of excited states of double-Λ hypernuclei.

Figure 12: Cross section at $\theta_{lab}=0°$ as a function of excitation energy in $^{16}_{\Lambda\Lambda}$C for the ^{16}O(K^-,K^+)$^{16}_{\Lambda\Lambda}$C* reaction at 1.1 GeV/c.

2.2 Study of ΛΛ Hypernuclei by Sequential Pionic Decays

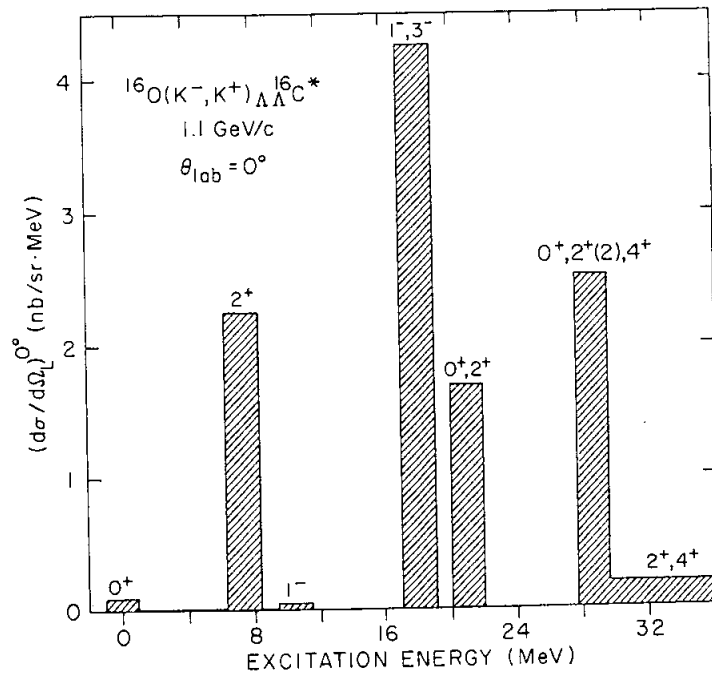Studies of double-Λ hypernuclei have attracted much interest, especially in connection with the existence of a predicted stable dibaryon, H, and the so far unsuccessful searches of H are certainly telling us something about quark systems in the non-perturbative regime. But the study of double-Λ hypernuclei also provides hitherto unavailable information concerning the Λ-Λ force, which is important in order to understand the baryon-baryon interaction in a unified way, and in particular its application to multi-strange systems, such as "strange matter". At nuclear densities only twice or three times that of normal nuclear matter, it is theoretically predicted that systems of multiple strangeness will appear. If true, this means that the inner part of the neutron stars would be composed of nucleons, hyperons, and leptons. Also of obvious related interest, is the strangeness content of the quark-gluon plasma. Thus it is important to determine the equation of state of strange nuclear matter, and for this one needs hyperon-nucleon and hyperon-hyperon interactions. This can best be done by validating baryon-baryon interaction models by studying $S=-1$ and -2 hypernuclei.

2.2.1 Introduction

Experimental studies on double-Λ hypernuclei are limited. In the 1960s two double-Λ hypernuclei were reported, showing sequential decay topologies in nuclear emulsion ($_{\Lambda\Lambda}^{10}$Be [5] and $_{\Lambda\Lambda}^{6}$He [6]). However the event in Ref. [6] is not convincing [7]. Recently new observations were made by the KEK-E176 and KEK-E373 experiments using the emulsion-counter hybrid detector system [8, 9], where Ξ^--particles were captured in emulsion with higher statistics than previously. The interpretation of the E176 event is not unique, however; i.e. either $_{\Lambda\Lambda}^{10}$Be or $_{\Lambda\Lambda}^{13}$B, and accordingly the extracted Λ-Λ interaction energy is either -4.9 ± 0.7 MeV (repulsive Λ-Λ interaction) or $+4.9 \pm 0.7$ MeV (attractive Λ-Λ interaction). Very recently it is claimed [9] that E373 found a uniquely identified double-Λ hypernucleus, $_{\Lambda\Lambda}^{6}$He, and determined the Λ-Λ interaction to be $1.01 \pm 0.20 \, _{-0.11}^{+0.18}$MeV, which is rather small compared to that claimed in past experiments. Another new method to study double-Λ hypernuclei with much more statistics was proposed and accepted at BNL-AGS as E906 [10], and in 1998 the physics run was carried out. We obtained about 0.9×10^{12} K^- on target, only about 45 % of the total requested irradiation of the E906 proposal. Nevertheless, that experiment demonstrated the usefulness of the technique and evidence of the production of $_{\Lambda\Lambda}^{4}$H has been obtained.

Based on the result, we are going to propose an extensive study of the double-Λ hypernuclei by this technique.

2.2.2 Experimental principle

The double strangeness and double charge exchange reaction, (K^-, K^+), near an incident momentum of 1.8 GeV/c, may be used to create double-Λ hypernuclei. In the simplest scenario (Fig. 13), the double-Λ hypernuclei could be produced by stopping Ξ^- and allowing these hyperons to interact with the target nuclei. The Ξ can be made via a quasi-free process through the (K^-, K^+) reaction, and then slowed down by energy loss in the production target. When essentially at rest a Ξ^- atom is formed, and the Ξ^- eventually absorbed by

the nucleus, such that $\Xi^- p \to \Lambda\Lambda$, i.e. the Ξ^- and a proton in the nucleus are converted into two Λ's by the strong interaction. Then the double-Λ compound state is formed with a "sticking" probability of more than $\sim 10\%$ [11]. It is also expected that the Ξ^- produced in the quasi-free process may be trapped in the same nucleus by the secondary reaction and, with some probability, two units of strangeness (eventually two Λ's) will be trapped in the same nucleus, albeit after emission of one or more nucleons, and form a double-Λ compound state. In any case, the compound state will subsequently decay into various hyperfragments containing one or two hyperons per fragment. Examples of such decays are $^{6}_{\Lambda\Lambda}$He and $^{4}_{\Lambda\Lambda}$H, and they can be identified by detecting characteristic mesonic-decay pions, in analogy to conventional $\beta - \gamma$ spectroscopy.

The $^{4}_{\Lambda\Lambda}$H case serves as an example. Formation of the $^{4}_{\Lambda\Lambda}$H hypernucleus can be identified by observing two characteristic pions from the successive pion decays ($^{4}_{\Lambda\Lambda}$H $\to$ $^{4}_{\Lambda}$He $+ \pi^-$ and $^{4}_{\Lambda}$He $\to$ ^{3}He $+ $ p $+ \pi^-$). The momentum of the π^-'s for the two-body decay mode will be monochromatic and that for three-body decay mode is also expected to be sufficiently narrow [12, 13]. From the momentum spectrum of pions in coincidence with pions of momentum ~ 97 MeV/c ($^{4}_{\Lambda}$He $\to$ ^{3}He $+ $ p $+ \pi^-$), we can determine the mass of $^{4}_{\Lambda\Lambda}$H. Note that the branching ratios of pion decay rates $\Gamma_{\pi^-}/\Gamma_{\mathrm{tot}}$ are known or expected to be large enough ; ~ 0.25 to ~ 0.52 for the present case[12, 13].

In E906 decay pions were detected in the Cylindrical Detector System CDS, which surrounds the target region (Fig. 14). The momentum resolution and the solid angle of the CDS were about 7 MeV/c FWHM for 100 MeV/c pions, and 65% of 4π, respectively. We used a ^{9}Be target sufficiently long in the beam direction so that there is a good chance for a quasi-free Ξ^- emitted in the forward direction to stop in the target material. According to a Monte Carlo simulation, we estimated about 4% of the Ξ^-'s will stop. The apparatus was installed at the 2 GeV/c K^- beam line(D6) at the AGS. This line typically delivers $(1 - 2) \times 10^6$ K^- /spill and a K/π ratio of about 0.72 at the momentum of 1.8 GeV/c with the usual beam-sharing conditions prevailing in fixed-target operation. The beam line and spectrometer drift chambers, particle ID detectors, and the trigger scintillators were used to identify the (K^-, K^+) reaction.

The CDS is constructed of three main components; the cylindrical drift chamber, CDC, a timing hodoscope, and a solenoidal magnet. A ^{9}Be target, 16 cm long, 5 cm wide, and 1.27 cm high, was centered within the CDS. The size of the DC is 298mm in radius and 920mm long. It consists of twelve readout layers; six axial and six stereo. The total number of cells is 576. In order to reduce the effect of multiple scattering as much as possible, low Z materials are selected for use inside the chamber. We employ 80 μm Al for the field wires, 20 μm W for the sense wires and a 50-50 mixture of helium and ethane as the chamber gas. An outer concentric hodoscope was used for timing and the trigger. As the hodoscope is inside the magnetic field, we employ a fine-mesh photomultiplier (Hamamatsu H6614) which is largely insensitive to this magnetic field. The size of the solenoid magnet is 1180 mm wide, 1180 mm high and 1280 mm long, and has a maximum field of 5 kGauss. The magnetic field has been checked with a NMR probe and the homogeneity of the field is within 0.5% for the entire CDC volume.

2.2.3 Proposed experiments

Based on the result of E906, we are going to propose a study of the double-Λ hypernuclei by means of decay-pion spectroscopy. In E961, we will identify $_{\Lambda\Lambda}^{4}$H by using a ^{7}Li target, and will determine the mass within 0.5 MeV accuracy. At the Joint Project, we expect a K-beam with an intensity of 5-10 times greater than the AGS and therefore we will be able to identify several weaker channels than $_{\Lambda\Lambda}^{4}$H case, e.g. $_{\Lambda\Lambda}^{6}$He. Another interesting possibility is that the Ξ-hypernuclei produced in the (K^-, K^+) reaction on ^{7}Li will decay to $_{\Lambda\Lambda}^{5}$H with a large branching ratio of about 90% [14] (Fig. 15). When we use heavier targets like ^{12}C, we can expect heavier double-Λ hypernuclei like $_{\Lambda\Lambda}^{10}$Be.

From the systematic study of the ground state mass of double-Λ hypernuclei, we will be able to deduce the Λ-Λ interaction with less ambiguity from the complications of nuclear structure. Moreover we can expect that a H-like structure, if any, will manifest itself in the structure of double-Λ hypernuclei, which can be studied at a future experiment with Ge-ball by observing gamma-rays from the double-Λ hypernuclei. Another interesting subject is the weak decay of the double-Λ hypernuclei; what is the total decay rate ? What kinds of the nonmesonic decay modes are available and what are their partial decay rates ? Are they affected by the co-existence of the H-like structure ? etc.

The detector to measure two pions will be an upgraded CDS, which can be a bit larger than the present one for a better momentum resolution and a better tracking capability. We will also install a vertex detector near the target (just above and below) to enable us to provide a much better vertex resolution in the target region. The overall momentum resolution will be better than 3 MeV/c for 100 MeV/c pions. The beam line system and the K^+ spectrometer will be the standard one for K1.8 beam line at the J-PARC.

2.3 γ-ray Spectroscopy of Double-Λ Hypernuclei

The γ-ray spectroscopy of double-Λ hypernuclei is one of the most important subjects to be pursued at the 50-GeV PS. Level structures of double-Λ hypernuclei give us information on the $\Lambda\Lambda$ interaction not only for the central force but also the spin-orbit force between two Λ's. They also provide information on the $\Lambda\Lambda$-ΞN coupling and a possible H-dibaryon-like correlation between two Λ's in a nucleus.

$_{\Lambda\Lambda}^{4}$H

As an example, we take $_{\Lambda\Lambda}^{4}$H, where nucleon spin-flip M1 transition, $0^+ \to 1^+$, can be observed around 3 MeV if both states are particle bound. $_{\Lambda\Lambda}^{4}$H are produced as a hyperfragment from the Li(K^-, K^+) reaction. We assume the following conditions to estimate the γ-ray yield:

· K^- beam intensity: 3.8×10^7 /spill(2×10^{14}ppp)
· PS cycle: 3.4 sec
· Beam time: 10 days
· Target: 20 g/cm^2 / 7 $\times 6 \times 10^{23}$

· Effective spectrometer solid angle: $\Omega_{eff} = 0.10$ sr
· Spectrometer tracking efficiency: $\epsilon_{sp} = 0.4$
· Ge detector efficiency: $\epsilon_{Ge} = 0.065$ at 3 MeV
· Ge detector live time: $\epsilon_{Ge\ live} = 0.6$

Here we use the intense K^- beam from the K1.8 beamline. We assume using a spectrometer having the acceptance ~ 0.10 sr for K^+ detection. The cross section for the quasi-free production of Ξ^- is taken to be 81 μb/sr, derived from ^{12}C data (99 μb/sr) and mass dependence ($A^{0.38}$) [15]. The formation probability of $^{4}_{\Lambda\Lambda}$H(0^+) state for quasi-free Ξ^- production events is assumed to be 0.06% using a theoretical estimate of the production rate for a double-Λ compound nucleus with ^{12}C target (0.3%) [16] and assuming the decay branching ratio of the compound nucleus to the $^{4}_{\Lambda\Lambda}$H(0^+) state of 20%.

With those assumptions, the expected yield for the γ-transition is 3100 counts. The background level is estimated to be 3×10^4 counts/100 keV. Thus the γ-ray peak would be clearly observed.

It is easy to identify the observed γ-ray peak as the one from the $M1(0^+ \to 1^+)$ transition in $^{4}_{\Lambda\Lambda}$H. From the double-charge-exchange Li(K^-, K^+) reaction only $Z = 0$ and $Z = 1$ fragments can be produced. With this condition, very limited (hyper-)nuclear species can be produced, among which only $^{4}_{\Lambda}$H and $^{4}_{\Lambda\Lambda}$H are expected to emit γ-rays. As we know the γ-ray energy of $^{4}_{\Lambda}$H is 1.04 MeV, we can safely assign the 3 MeV γ-ray to the $M1(0^+ \to 1^+)$ transition in $^{4}_{\Lambda\Lambda}$H. It is noted that when we take into account weak decays of (double-)Λ hypernuclei, single-Λ hypernuclei of $Z = 2$ and normal nuclei of $Z = 2$ and 3 can also be produced, but all possible γ-transitions in those (hyper-)nuclei are known.

Furthermore, this γ-ray assignment can be supported by taking γ-γ coincidence. The ground state of $^{4}_{\Lambda\Lambda}$H (1^+) is expected to decay by

$$^{4}_{\Lambda\Lambda}\text{H} \to {}^{4}_{\Lambda}\text{H}({}^{4}_{\Lambda}\text{He}) + \pi^0(\pi^-)$$

with large branching ratios (~ 0.5 in total). Here, the excited states (1^+) of $^{4}_{\Lambda}$H($^{4}_{\Lambda}$He) are favorably populated over the ground states (0^+), because the spin non-flip amplitude is much larger than the spin-flip amplitude in the mesonic weak decay [17]. Therefore, we can detect 1.1 MeV γ-rays from $^{4}_{\Lambda}$H($^{4}_{\Lambda}$He) in coincidence with the $^{4}_{\Lambda\Lambda}$H γ-rays. Using the branching ratio above and the γ-ray detection efficiency, we expect 110 counts for the γ-γ coincidence events.

$^{13}_{\Lambda\Lambda}$B

One of the most important experiments for double-Λ hypernuclei is to detect E1($p_\Lambda \to s_\Lambda$) transitions of $^{13}_{\Lambda\Lambda}$B. The energy difference of E1 γ transitions of $p_{3/2\ \Lambda}s_\Lambda \to s_\Lambda s_\Lambda$ and $p_{1/2\ \Lambda}s_\Lambda \to s_\Lambda s_\Lambda$ provides valuable information on the spin-orbit force between two Λ's. $^{13}_{\Lambda\Lambda}$B was produced in the KEK E176 experiment from Ξ^- absorption in emulsion (probablly on ^{14}N), although another assignment to $^{10}_{\Lambda\Lambda}$Be cannot be excluded for this double hypernuclear event [18]. According to the E176 result, the yield of $^{13}_{\Lambda\Lambda}$B, including the π^- mesonic decay branching ratio, may be of the order of one out of 78 stopped Ξ^- from about 800 events of the quasi-free Ξ^- prodiction in the (K^-, K^+) reaction. This corresponds to the E1($p_\Lambda \to$

s_Λ) gamma-ray yield of the order of 100 in 10 days' beamtime at the 50-GeV PS. So this experiment seems to be feasible, although more information on the production and decay of $^{13}_{\Lambda\Lambda}$B is necessary.

References

[1] J. Doornbos, KEK Report 97-5 (1997).

[2] T. Koike and Y. Akaishi, Genshikaku-Kenkyu 41 (19xx) 87.

[3] K.S. Myint and Y. Akaishi, Prog. Theor. Phys. Suppl. 117 (1994) 251.

[4] A.J. Baltz, C.B. Dover, and D.J. Millener, Phys. Lett. 123B (1983) 9.

[5] M. Danysz et al., Nucl. Phys. 49 (1963) 121.

[6] P.J. Prowse, Phys. Rev. Lett. 17 (1966) 782.

[7] R.H. Dalitz et al., Proc. R. Soc. Lond. A426 (1989) 1.

[8] S. Aoki et al., Prog. Theor. Phys. 85 (1991) 1287.

[9] H .Takahashi et al., Phys. Rev. Lett. **87**, 212502-1 (2001).

[10] T. Fukuda and R.E. Chrien, AGS proposal E906 (1994).

[11] K. Nakazawa, *in* Proc. of the 23rd INS Int. Symp. on Nuclear and Particle Physics with Meson Beams in the 1 GeV/c Region, eds. S. Sugimoto and O. Hashimoto (Universal Academy Press, Tokyo, 1995), p. 261.

[12] Izumi Kumagai-Fuse, Shigeto Okabe, and Yoshinori Akaishi, Phys. Rev. C54 (1996) 2843.

[13] Y. Yamamoto, M. Wakai, T. Motoba and T. Fukuda, Nucl. Phys. A625 (1997) 107; Y. Yamamoto, Nucl. Phys. A639 (1998) 393c.

[14] I. Kumagai-Fuse and Y. Akaishi, Phys. Rev. 54 (1996) R24.

[15] T. Iijima *et al.*, Nucl. Phys. **A546** (1992) 588.

[16] Y. Yamamoto, M. Wakai, T. Fukuda, M. Sano, Prog. Theor. Phys. **88** (1992) 1163.

[17] T. Motoba and K. Itonaga, Prog. Theor. Phys. Suppl. **117** (1994) 477.

[18] S. Aoki *et al.*, Prog. Theor. Phys. **85** (1991) 951; K. Imai, Nucl. Phys. A547 (1992) 199.

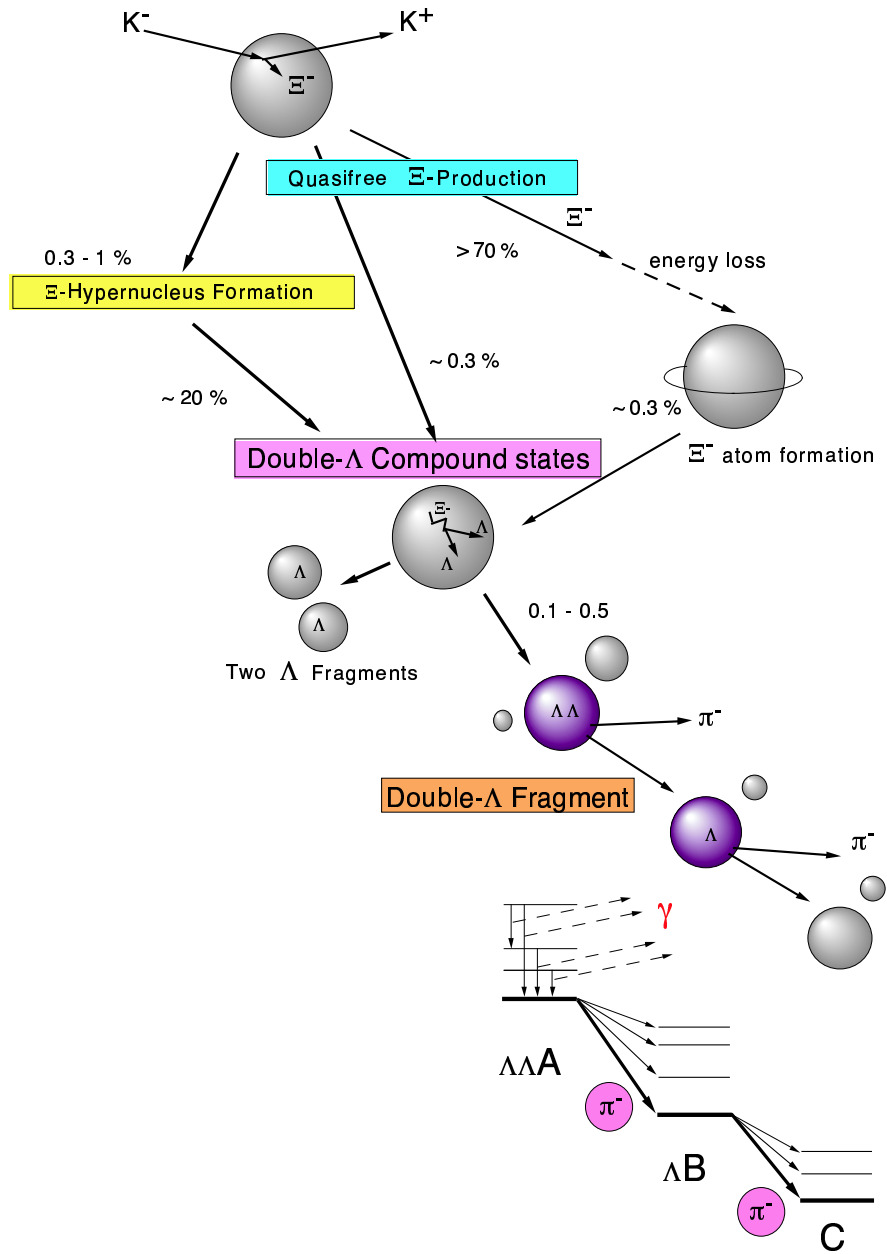Figure 13: A possible scenario to produce and detect double-Λ hypernuclei in the (K^-, K^+) reaction.
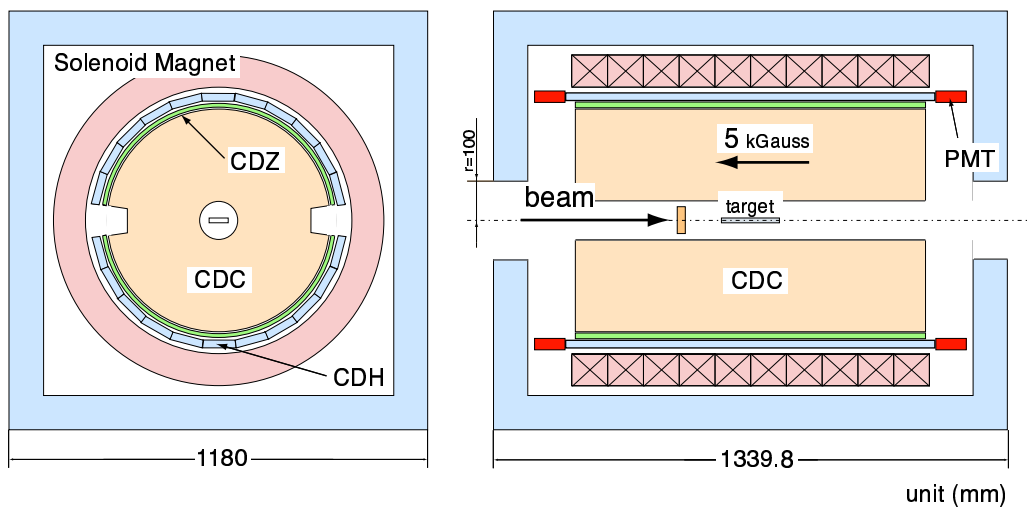
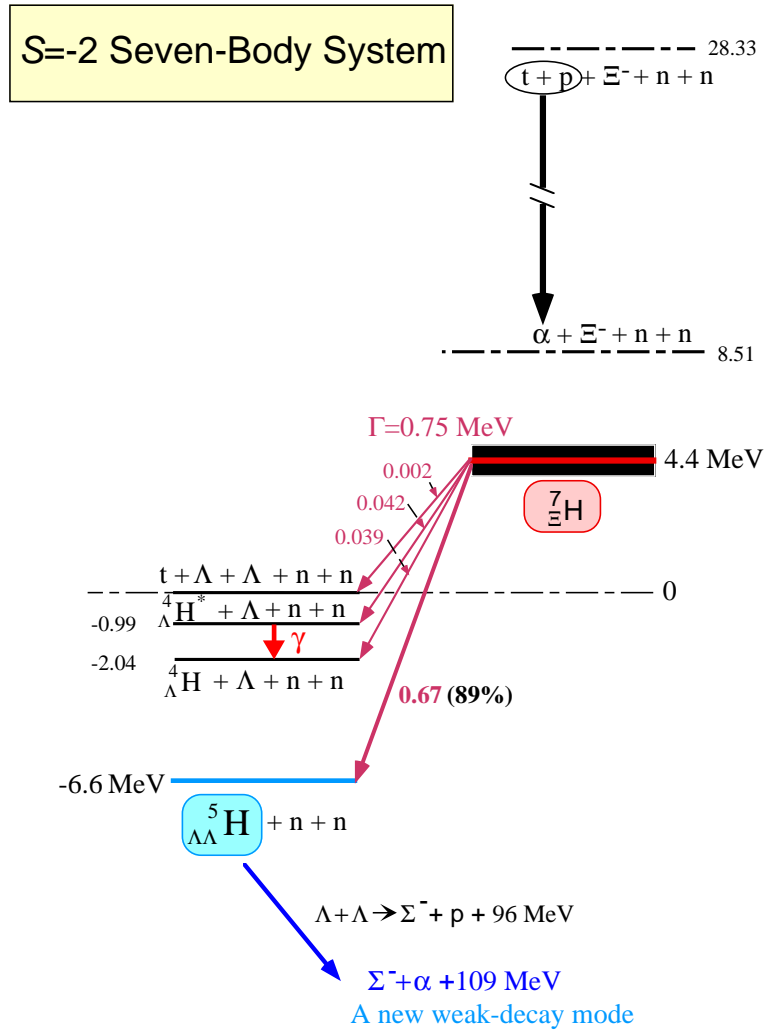Figure 14: A schematic drawing of the Cylindrical Detector System (CDS).

Figure 15: The energy levels of the $S=-2$ five-body system.

3   Proposal for Hypernuclear γ-ray Spectroscopy

3.1   Introduction

Precision γ spectroscopy using germanium (Ge) detectors, which is one of the most powerful means to study nuclear structure, has recently been introduced to hypernuclear physics. In 1998 we constructed Hyperball, a large-acceptance Ge detector array equipped with fast readout electronics and succeeded in observing hypernuclear γ rays for the first time with Ge detectors [1, 2, 3]. The energy resolution of hypernuclear levels has been drastically improved from 1–2 MeV (FWHM) into a few keV (FWHM). Since then we have observed more than fifteen γ transitions from several Λ hypernuclei, $^{7}_{\Lambda}$Li, $^{9}_{\Lambda}$Be, $^{11}_{\Lambda}$B, $^{15}_{\Lambda}$N and $^{16}_{\Lambda}$O, in KEK E419, E509, E518 and BNL E930 experiments [2, 3, 4, 5, 6]. Precision hypernuclear γ spectroscopy has been established as a new frontier in strangeness nuclear physics.

At the 50 GeV PS, we will be able investigate almost all bound-state levels of various hypernuclei ranging from $^{4}_{\Lambda}$He to $^{208}_{\Lambda}$Pb. Measurements of angular correlations and polarizations of γ-rays allow us to assign spin-parities of states. We can thus clarify detailed level schemes of various hypernuclei and make "Table of Hyper-Isotopes" book, a hypernuclear version of the "Table of isotopes". Such data will be used to extract properties and strengths of the YN and YY interactions and to discuss nuclear structure change induced by a Λ as an impurity. Transition probabilities of $B(E2)$ and $B(M1)$ will be also measured for many hypernuclear transitions. $B(E2)$'s provide information on the size and deformation of hypernuclei, which are expected to be changed from those of normal nuclei because of a Λ particle. $B(M1)$'s allow us to extract a g-factor value of a Λ in a nucleus which may be modified from the free-space value.

The physics subjects which can be pursued by precision hypernuclear γ spectroscopy are classified into

1. YN interactions,

2. Impurity nuclear physics, and

3. Medium effect of baryons.

In the following, we describe more about the three physics subjects

3.2   Physics subjects

3.2.1   YN interaction

From detailed hypernuclear level structure, we can establish the ΛN spin-dependent (spin-spin, spin-orbit, and tensor forces) interaction strengths, and then investigate ΣN-ΛN coupling force, charge symmetry breaking, and odd-state interactions.

Experimental information on these characteristics of the ΛN interaction plays an essential role to discriminate and improve baryon-baryon interaction models, not only those based on meson-exchange picture but also those including quark-gluon degree of freedom, toward unified understanding of the baryon-baryon interactions. For example, the very small Λ spin-orbit force established by recent γ spectroscopy experiments of $^{9}_{\Lambda}$Be [4] and $^{13}_{\Lambda}$C [7]

seem to suggest that the quark-gluon picture is valid for the spin-orbit force. In addition, understanding of the YN and YY interactions is necessary to describe high density nuclear matter containing hyperons.

Spin-dependent forces   The ΛN interaction can be expressed as

$$V_{\Lambda N} = V_0(r) + V_\sigma \mathbf{s}_N \mathbf{s}_\Lambda + V_\Lambda \mathbf{l}_{N\Lambda}\mathbf{s}_\Lambda + V_N \mathbf{l}_{N\Lambda}\mathbf{s}_N + V_T[3(\boldsymbol{\sigma}_N \hat{\mathbf{r}})(\boldsymbol{\sigma}_\Lambda \hat{\mathbf{r}}) - \boldsymbol{\sigma}_N \boldsymbol{\sigma}_\Lambda] \tag{1}$$

In shell-model description of p-shell hyeprnuclei, the effective $s_\Lambda p_N$ (and $p_\Lambda s_N$) interactions have five radial integrals corresponding to each of the five terms in Eq. 1, denoted by $\bar{V}$, Δ, S_Λ, S_N and T, respectively [8, 9]. These integrals can be determined phenomenologically from low-lying level structure of p-shell hypernuclei. Before we started the hypernuclear γ spectroscopy project with Hyperball, the spin-dependent terms (Δ, S_Λ, S_N and T) were not well known; the available hypernuclear data were not of sufficient quality and quantity to unambiguously extract them. The study of these ΛN spin-dependent interactions have recently been started using Hyperball. In KEK E419 and BNL E930, we observed several γ transitions in $^7_\Lambda$Li, $^9_\Lambda$Be, $^{15}_\Lambda$N, and $^{16}_\Lambda$O, and the parameters of Δ, S_Λ, S_N are determined [2, 4], and T will be soon obtained from $^{15}_\Lambda$N and $^{16}_\Lambda$O data from E930 [6].

Three-body force   However, the level energies of hypernuclei might not be able to be understood by those two-body effective interactions because of possible effect of the ΛNN three-body force due to intermediate Σ states (see Fig. 16). It was recently understood that the three-body force give rise to a large effect to binding energies of the 1^+ and 0^+ states of $A = 4$ hypernuclei [10].
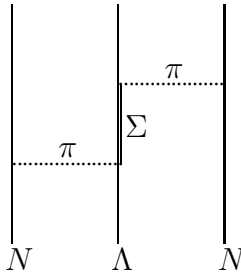
Figure 16: A diagram for the ΛNN three-body force due to intermediate Σ states introduced by ΛN-ΣN couplings.

The three-body force caused by the diagram in Fig. 16 is expected to be stronger than the $3N$ force including the intermediate Δ states, since the Σ particle in intermediate state is only 80 MeV heavier than the Λ particle compared to the 300 MeV difference in the case of nucleon and Δ. In addition, since the ΛNN force is mediated by two-pion exchange while one-pion exchange between a Λ and a nucleon is forbidden by isospin conservation, relative importance of the ΛNN force to the ΛN force is expected to be large. Therefore, study of the ΛNN three-body force as well as the two-body force is of great importance to understand the structure of hypernuclei. It is also noted that the three-body force is a pure many body

effect, and thus the importance will not be reduced even if the free ΛN interaction is well studied by elastic scattering experiments.

The ΛNN force, which is not renormalizable into two-body effective ΛN interaction, changes level energies of hypernuclei so that they cannot be expressed with the five ΛN two-body effective interactions in Eq. 1. Therefore, when we determine the parameter set for the spin-dependent forces (Δ, S_Λ, S_N, and T) redundantly, we can see effects of the ΛNN force by consistency of those parameters obtained from various hypernuclear states. Actually, our data of $^{10}_\Lambda$B($T = 1/2$) taken in E930 cannot be explained by the parameter set ($\Delta = 0.5, |S_\Lambda| < 0.03, S_N = -0.4$ MeV) which was determined from the $^7_\Lambda$Li($T = 0$) and $^9_\Lambda$Be($T = 0$) data. To obtain more information of the ΛNN force, plenty of hypernuclear data, particularly of states with non-zero isospin, are required, because the effect of the three-body force is expected to be large for non-zero isospin states due to the isospin of the intermediate Σ. Plenty of hypernuclear data will also help us discuss the two-body interactions more precisely, because it enables us to reduce uncertainties of structure of each nucleus, such as nuclear size or clustering feature.

Charge symmetry breaking Another important subject in the study of ΛN interaction is the charge symmetry breaking (CSB) effect. Since a Λ has no isospin and no charge, the Λp and Λn interactions are the same if the charge symmetry holds exactly. However, the Λ binding energies of the lightest mirror pair of hypernuclei, $^4_\Lambda$H and $^4_\Lambda$He, are known to have a large difference, and it is implied that the Λp interaction is more attractive than the Λn interaction. This effect can be precisely investigated from level structure of various mirror hypernuclei, rather than by YN scattering experiments where precise Λn scattering experiments are almost impossible.

As for the origin of such large CSB, no conclusive remark is obtained yet, although several mechanisms such as Λ-Σ^0 mixing and ΛN-ΣN coupling are proposed. In order to answer the question, to investigate the spin-dependence of the CSB interaction is very important. For example, Λ-Σ^0 mixing model expects a CSB potential similar to that of one-pion exchange, which includes spin-spin and tensor forces, while it was suggested that the CSB potential is almost spin independent based on the $A = 4$ hypernuclear data [11]. If the CSB potential is really spin independent, Λ-Σ^0 mixing is not a significant source of the CSB.

Another candidate for the origin of CSB is the ΛN-ΣN coupling effect; CSB occurs through the mass difference of Σ^+, Σ^0, and Σ^- which is some 8 MeV or about 10% of the Σ-Λ mass difference. As described above, this mechanism also plays an essential role for the ΛNN three-body force. This fact implies that the CSB might appear in the ΛNN force as well as in the ΛN force.

Systematic study of various pairs of mirror hypernuclei to investigate the spin-dependence and possible three-body force components in CSB interaction is indispensable to clarify the characteristics and thus the origin of the CSB interaction.

Odd-state interaction The 30 MeV potential depth of a Λ in nuclear matter is governed by both of even state (S wave) and odd-state (P wave) ΛN interactions [12]. Various one-boson-exchange baryon-baryon interaction models by Nijmegen and Jürich groups roughly

reproduce the 30 MeV depth, but the relative contribution between the even and the odd state interactions is different; while the oldest ND model has an attractive odd-state force, the NSC97f model, successfully reproducing various hypernuclear data, has a repulsive odd-state force which is inconsistent with the $^{13}_{\Lambda}$C data [13]. Since the odd-state interaction has a larger contribution in higher density nuclear matter, hyperon mixing expected in neutron stars cannot be properly described without knowledge of the ΛN odd-state force [12].

We aim at studying the strengths of the spin-averaged part and the spin-spin part of the odd-state central force. The detailed level structure of p_{Λ} states in hypernuclei will allow us to separately extract the strengths of these odd-state forces. Since the p_{Λ} levels are usually particle unbound for light ($A < 50$) hypernuclei, we need to investigate medium and heavy hypernuclei such as $^{89}_{\Lambda}$Y and $^{208}_{\Lambda}$Pb.

3.2.2 Impurity nuclear physics

Since hyperons are free from Pauli effect and feel nuclear forces different from those nucleons do in a nucleus, only one (or two) hyperon(s) introduced in a nucleus may give rise to various changes of the nuclear structure, such as changes of the size and the shape, change of the cluster structure, emergence of new symmetries, change of collective motions, *etc.* Level schemes and $B(E2)$'s of Λ hypernuclei studied by γ spectroscopy will reveal such interesting phenomena, and a new field to be called "impurity nuclear physics" will be exploited.

In KEK E419, we measured the lifetime of the $\frac{5}{2}^+$ state of $^7_{\Lambda}$Li by analyzing the $E2(\frac{5}{2}^+\to\frac{1}{2}^+)$ γ-ray peak shape which is partly Doppler-broadened according to the lifetime of $^7_{\Lambda}$Li($\frac{5}{2}^+$) and the stopping time of the recoiling $^7_{\Lambda}$Li($\frac{5}{2}^+$) in target material. The high resolution of Ge detectors enabled us to apply this method called Doppler-shift attenuation method (DSAM) for the first time. From the measured lifetime we derived $B(E2; \frac{5}{2}^+\to\frac{1}{2}^+)$ [3]. By comparing it with the $B(E2)$ of the corresponding transition in the core nucleus, namely, $B(E2; 3^+\to1^+)$ of ^{6}Li, the nuclear size was found to be contracted by 19$\pm$4% due to addition of a Λ in the $0s$ orbit. Such a nuclear shrinkage is a general property of hypernuclei, which was first predicted by Motoba *et al.* in 1983 [14] and then precisely calculated by Hiyama *et al.*[15]

Such a nuclear structure change induced by a Λ may appear in various hypernuclei [16] as described in Sect. 3.5.2 and 3.8.1. In particular, drastic changes of nuclear structure are expected when a Λ is implanted into neutron-rich hypernuclei having neutron skins or halos.

3.2.3 Medium effect of baryons – $B(M1)$ measurement

Using hyperons free from Pauli effect, we can investigate possible modification of baryons in nuclear matter through magnetic moments of hyperons in a nucleus.

Magnetic moments of baryons can be well described by the picture of constituent quark models in which each constituent quark has a magnetic moment of a Dirac particle having a constituent quark mass. If the mass (or the size) of a baryon is changed in a nucleus by possible partial restoration of chiral symmetry, the magnetic moment of the baryon may be changed in a nucleus. A Λ particle in a hypernucleus is the best probe to see whether such an effect really exists or not.

Possible change of the magnetic moment of a Λ in a nucleus has attracted attention of nuclear physicist. It was first pointed out [17] that Pauli effect in the quark level, if it exists, may modify a hyperon in a hypernucleus and change its magnetic moment. Then a calculation with the quark cluster model [18] showed that the "quark exchange current" between two baryons at a short distance changes the magnetic moment, of which effect depends on the confinement size of the hyperon in the nucleus.

Direct measurement of hypernuclear magnetic moments is extremely difficult because of its short lifetime for spin precession. A new approach using heavy ion beams is also being proposed. Here we propose to derive a g-factor of Λ in the nucleus from a probability ($B(M1)$ value) of a spin-flip $M1$ transition between hypernuclear spin-doublet states (see Fig. 17). In the weak coupling limit between a Λ and a core nucleus, the $B(M1)$ is expressed as [8]

$$B(M1) \propto | <\phi_{lo}|\mu^z|\phi_{up}> |^2 = | <\phi_{lo}|g_N J_N^z + g_\Lambda J_\Lambda^z|\phi_{up}> |^2 \propto (g_N - g_\Lambda)^2$$

where g_N and g_Λ denote effective g-factors of the core nucleus and the Λ, and J_N^z and J_Λ^z denote their spin operators, respectively. Here the space components of the wavefunctions of the lower and upper states of the doublet (ϕ_{lo}, ϕ_{up}) are assumed to be identical.

Transition probabilities such as $B(M1)$ are derived from lifetimes of excited states, using the Doppler shift attenuation method described above, or a newly proposed method called "γ-weak coincidence method" described in Sect. 3.10.2.

In this study, effect of the meson exchange current between a Λ and a nucleon has to be considered. The meson exchange current is expected to be totally different from the NN case, because in the ΛN interaction one-pion exchange is forbidden but Λ-Σ coupling makes another effect. $B(M1)$ values and magnetic moments of several s, p-shell hypernuclei were calculated in order to investigate such effects [19]. These effects were found to be of the order of several %. For example, $B(M1)$ of $^7_\Lambda$Li($3/2^+ \rightarrow 1/2^+$) is reduced by 7%. Accurate measurement of $B(M1)$ for various hypernuclei will also reveal the effect of the meson exchange current.

3.3 Plans of experiments

The experimental subjects for precision γ spectroscopy are listed below. They are classified by the physics motivations and experimental methods.

(1) Complete study of light ($A < 30$) Λ hypernuclei with (K^-,π^-) reaction. (1-a) Survey experiment. (1-b) Detailed study for several hypernuclei.

(2) Systematic study of medium and heavy Λ hypernuclei with (K^-,π^-) reaction

(3) Study of hyperfragments including n-rich hypernuclei with K^--in-beam or stopped K^- method

(4) Study of n-rich and mirror hypernuclei with (K^-,π^0) reaction

(5) $B(M1)$ measurements with (K^-,π^-) and (π^+,K^+) reactions using Doppler shift attenuation method

(6) $B(M1)$ measurements using γ-weak coincidence method

Table 4: Requirements of beam and apparatus of planned experiments. Listed are the reaction used and beam momentum, the beam line used, additional apparatus except for Hyperball, and necessary beam intensity.

	Subject	Reaction, P_{beam} (GeV/c)	Beam line	Apparatus	Intensity
(1-a)	Light (survey)	$(K^-,\pi^-\gamma)$ 1.1 and 0.8	K1.1	MS	*
(1-b)	(detailed)	$(K^-,\pi^-\gamma)$ 1.1 and 0.8	K1.1	MS	**
(2)	Medium, heavy	$(K^-,\pi^-\gamma)$ 1.8 (–0.8)	K1.8 (K1.1)	MS	**
(3)	Hyperfragments	$(K^-,\gamma\ (\pi^-))$ 0.8–0.6	K1.1	(simple MS)	*
(4)	Mirror/n-rich	$(K^-,\pi^0\gamma)$ 1.1 and 0.8	K1.1	π^0 Spectrometer	***
(5)	$B(M1)$ DSAM	$(\pi^+,K^+\gamma)$ 1.05	K1.1(K1.8)	MS	*
		$(K^-,\pi^-\gamma)$ 1.1	K1.1	MS	**
(6)	$B(M1)$ γ-weak	$(K^-,\pi^-\gamma$ weak) 1.1 or 0.8	K1.1	MS + decay arm	***

MS magnetic spectrometer
* $< 1/10$ of full proton beam
**   1/10–1/2 of full proton beam
*** $> 1/2$ of full proton beam

The purposes of the experiments (1)–(4) are to study YN interactions and impurity effect from various Λ hypernuclear structure, while the experiments (5) and (6) study nuclear medium effect of baryons through g-factor of a Λ in various nuclei. Table 4 summarizes the requirements of the beam and additional apparatus of each experiment.

In the early stage with low proton beam intensity (less than 1/10 of the full beam), we begin with "easy" experiments which are regarded as extensions or straightforward development of our previous experiments already done at KEK and BNL (E419, E930, E509, E518). At first we study various light hypernuclei with (K^-,π^-) reaction (1-a) (development of E930) and with in-beam or stopped K^- method (3) (development of E509/E930). The $B(M1)$ measurements of light hypernuclei with the (π^+,K^+) reaction (5) (development of E518) can also run in the very early stage,

When more proton beam intensity is available (1/10–1/2 of the full beam), we plan complete study of all possible light hypernuclei, in which γ-γ coincidence technique will be also applied to several important hypernuclei (1-b). The $B(M1)$ measurements with the (K^-,π^-) reaction is also possible with this beam intensity.

When the full beam is available, we construct a π^0 spectrometer and use the (K^-,π^0) reaction for n-rich hypernuclei and mirror hypernuclei (4). For some of these hypernuclei, the impurity effect will be also investigated by measuring $B(E2)$ values. The $B(M1)$ measurements with γ-weak coincidence method (6) is possible with the full beam intensity, combining the decay arm detectors and the fully upgraded Hyperball.

After all these proposed experiments, γ-ray spectroscopy will be mostly pursued for double hypernuclei described in the previous section.

3.4   Method and Setup

3.4.1   Requirement of beam

In most of the proposed experiments, we use the (K^-,π^-) reaction both at 1.1 GeV/c and 0.8 GeV/c. The experiment with both beam momenta is necessary to reconstruct the level

scheme. The 1.1 GeV/c (K^-, π^-) reaction has a very large spin-flip amplitude; as shown in Fig. 18, the elementary reaction $(K^-n \to \Lambda\pi^-)$ has 100% polarization at K^- momentum of 1.1 GeV/c and pion scattering angle of 10^0, which indicates that the spin-flip amplitude is large equally to the non-spin-flip amplitude in this condition. Consequently, efficient population of the spin-flip partner in the hypernuclear doublet is possible only with 1.1 GeV/c K^- beam. On the other hand, Fig. 18 shows that the K^- momentum of 0.8 GeV/c has a large cross section to produce Λ with completely no spin-flip amplitude. In addition, the recoil momentum is small enough ($\sim$50 MeV/c at 0^0) to avoid Doppler broadening of γ rays from hypernuclei.

We need a beam line optimized to 1.1 GeV/c kaons (K1.1). It should provide high-intensity (1×10^7/sec) and pure ($K^-/\pi^- > 1$) kaon beam. Beam purity is important because counting rates and radiation damage of Ge detectors due to unwanted pions decrease experimental efficiency. Therefore, construction of a double-stage-separator beam line independent of the K1.8 beam line is preferable. Because of budgetary limitation, the K1.1 line with a single-stage separator branched from the K1.8 beam line is proposed as our minimum request. This beam line can be well used in the early stage, but the full intensity kaon beam may not be able to be accepted because of a worse K/π ratio.

In the $B(M1)$ measurement (5), the (π^+, K^+) reaction will be sometimes used, as in E518, in order to utilize its large momentum transfer. In this case we use 1.05 GeV/c π^+ beam from the K1.1 or K1.8 beam line. The beam intensity limit of 10^7/sec is 100 times lower than the full pion beam intensity of these beam lines, and thus it can run in the very early stage.

In the experiment (2), we need 1.8 GeV/c K^- beam at the K1.8 beam line.

3.4.2 Spectrometers

In the experiment (1),(2),(5),(6), the incident K^- (or π^+) beam and the secondary π^- (or K^+) have to be momentum-analyzed in the event-by-event basis with the resolution of $\Delta p/p < 0.2\%$ in order to obtain hypernuclear mass resolution better than 3 MeV FWHM for selection of bound states.

The beam momentum can be analyzed with the beam spectrometer magnet used at the present K6 line ("Kamae magnet", 1.2 GeV/c at maximum). The secondary particle analyzer should cover the momentum up to 1.05 GeV/c and had better have a large acceptance of > 50 msr so that various hypernuclear states of different angular momentum transfer can be populated without changing the magnet setting.

For the secondary particles, the SKS spectrometer is best suited, but in the beginning when the SKS is used at the K1.8 beam line, we use the existing SPESII spectrometer although the acceptance is smaller (~ 20 msr). Since the maximum momentum of SPESII is slightly lower than we need for the 1.1 GeV/c (K^-, π^-) reaction, the magnet arrangement has to be modified. In the future, we plan to request a budget to construct a new spectrometer having a large acceptance (> 50 msr) and a moderate resolution ($< 0.2\%$), or to construct a new dedicated spectrometer for K1.8 and use the SKS for γ spectroscopy at K1.1.

Figure 19 illustrates a planned setup with SPESII at K1.1. We install a set of detectors for the beam and secondary particle spectrometers similar to those in the present K6/SKS

system. In the beginning with the total beam intensity less than 10^7/sec, we use 1-mm pitch MWPC's for the tracking device in the beam (BC1-BC4, SC1-SC2) instead of the present 2.5 mm pitch drift chambers. When the full beam intensity is available, the tracking devices should be operated at a beam rate of 2×10^7 /sec, 5 times more than the present K6 case. Then we need scintillation fiber (SCIFI) hodoscopes (0.5-1 mm pitch) for BC1-BC2, 0.5 mm pitch MWPC's for BC3-BC4 and SC1-SC2, and 3mm-pitch large-size drift chambers for SC3-SC4. The 0.5 mm-pitch MWPC's are under development at present. The other detectors are easily realized. A fast DAQ system has to be prepared which works at about 2000 trigger/sec $\times$ 1kB/event.

In the K^--in-beam experiment (3), we only need to identify π^- emission and to measure the pion momentum very roughly ($\sim$0.1 GeV/c resolution), according to our experience at E930 where we used the 48D48 magnet only to identify π^- emission (see Sec. 3.7). Here a large acceptance rectangular magnet such as Kurama or Tokiwa is suited. As this experiment does not require track reconstruction, we only need plastic counter hodoscopes at the exit of the magnet as well as Cerenkov counters and drift chambers only around the target. Since the detector setup is very simple and cheap, this experiment can be carried out even under a severe lack of budget. In the case of the stopped K^- method, which is effective if the beam intensity is very low, we do not need any magnet and tracking detectors.

In the (K^-,π^0) experiment (4), we need to construct π^0 spectrometer similar to the one (NMS) used at BNL E907/931 [20]. It consists of an array of CsI or GSO counters to detect 2γ's and sustains a solid angle of about 10 msr for π^0. It should have an energy resolution better than 2 MeV FWHM at 0.7 GeV/c. Combined with the same beam tracking setup as in (1),(2),(5),(6), the hypernuclear mass has to be measured with < 3 MeV resolution.

In the γ-weak coincidence experiment (6), we also need "decay arm" detectors which measure the energy, track, and timing of protons and π^-'s emitted from weak decays of Λ hypernuclei. Details are described in Sect. 3.10.2.

3.4.3 Upgraded Hyperball

The present Hyperball consists of fourteen sets of coaxial N-type Ge detectors (relative efficiency of 60% for each) equipped with fast readout electronics. Each Ge crystal is surrounded by BGO scintillation counters to suppress background from Compton scattering and high energy γ rays from π^0.

At present, the Ge detectors and the BGO counters of Hyperball can accept 4×10^6 beam particles per second when installed at 15 cm from 20 g/cm^2-thick target. The maximum beam intensity at the 50 GeV PS will be 2×10^7 beam particles per second for 1.1 GeV/c K^- beam at K1.1. Therefore, the readout electronics should be further improved. The dead time of Ge detectors is caused by pile-up of signals and recovery time after preamplifier reset. We are developing a new readout method with high-resolution waveform digitizers, which allows us to decompose pile-up signals in offline analysis. A lower-gain preamplifier is also necessary to reduce the rate of preamplifier reset and to decrease dead time caused by reset. We expect that the capability for high counting rate will be improved by a factor of 5 or more in 3–4 years.

As for the BGO counters surrounding each Ge crystal, the slow decay time of scintillation

makes it difficult to use them with beam intensity higher than 5×10^6 particle/sec. We are developing new counters made of fast scintillators such as GSO, LSO, or PWO so that we can accept more than 10 times higher beam intensity.

In addition, we plan to increase the number of Ge detectors as far as the budget permits. In our best possible design, we use 14 sets of segmented Super-Clover Ge detectors, which has recently become commercially available. One detector set consists of four Ge crystals of $7\text{cm}\phi \times 14$ cm, and the electronode of each crystal is segmented into 4 readout channels. Such a fine segmentation results in better Doppler shift correction. The detectors are installed so that the crystal surface is located at 20–25 cm from the target. This distance is necessary for counting rate of the detectors as well as for the Doppler shift correction. The Ge crystals cover about 40% of the total solid angle. The Ge detector system has a photo-peak efficiency of 12% at 1 MeV in total, as shown in Fig. 21. The construction of the upgraded Hyperball will hopefully be funded in universities.
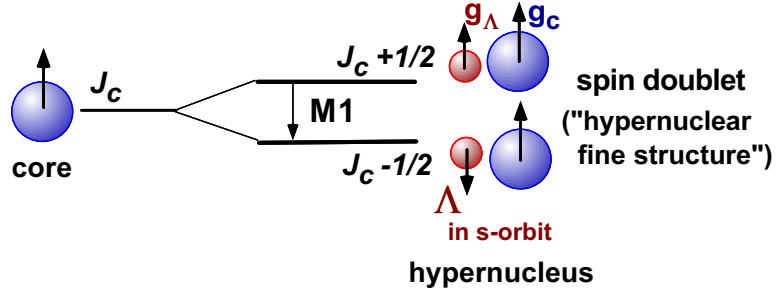
Figure 17: Spin doublet and spin-flip $M1$ transition in a hypernucleus. When a Λ is coupled to the core nucleus with spin J_c, the level is split into a doublet$(J_c+1/2, J_c-1/2)$. The spin flip of the Λ gives rise to the $M1$ transition from the upper to the lower state in the doublet, and its probability $B(M1)$ is proportional to $(g_c - g_\Lambda)^2$, where g_c and g_Λ denote g-factors of the core nucleus and a Λ particle inside a nucleus (see text).
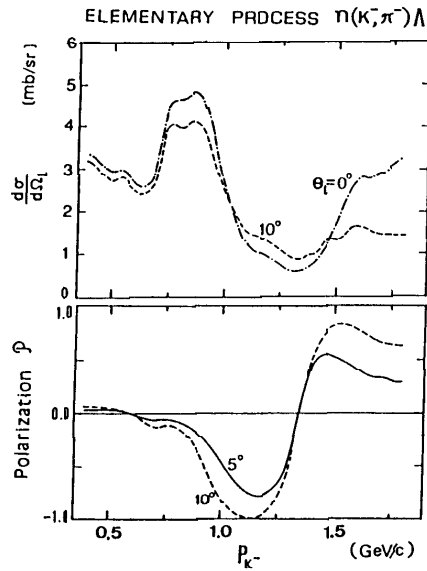
Figure 18: Cross section and polarization of the $K^- n \to \Lambda \pi^-$ reaction as a function of K^- momentum.
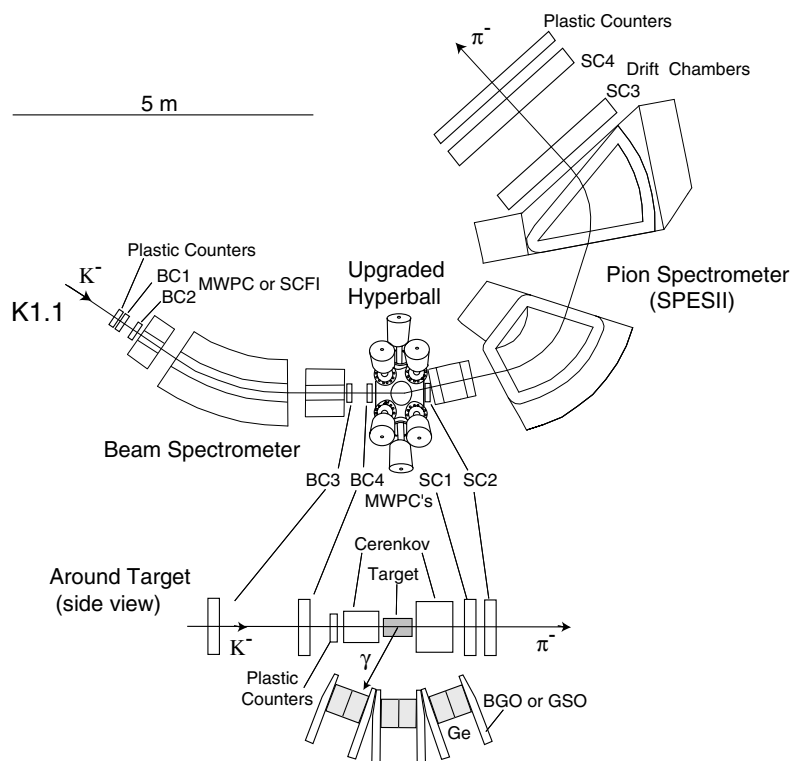
Figure 19: Setup for hypernuclear γ-spectroscopy experiments with the (K^-,π^-) reaction at K1.1 beam line.
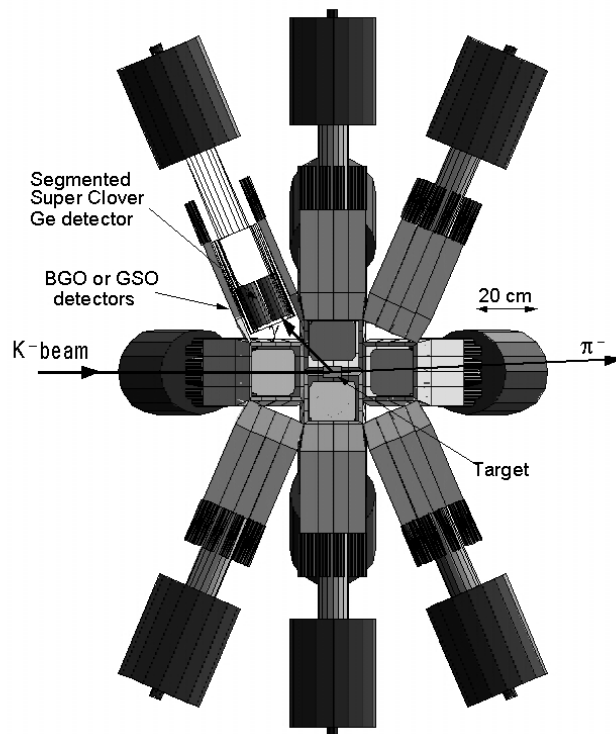
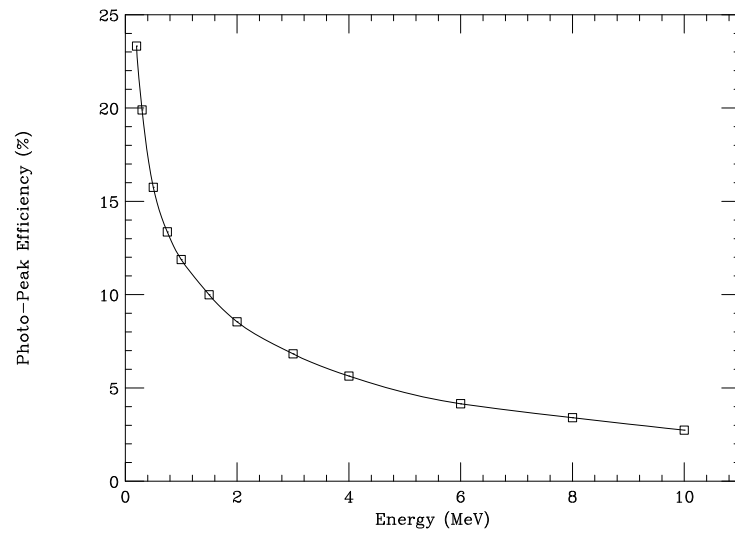Figure 20: Ge detector system for hypernuclear γ spectroscopy.

Figure 21: Absolute photo-peak efficiency of the Ge detector system which consists of 14 sets of Segmented Super Clover Ge detectors.

3.5 Spectroscopy of Light Hypernuclei by (K^-,π^-) (1)

We aim at complete study of precision γ spectroscopy for all the possible hypernuclei of $A < 30$, namely, $^4_\Lambda$He, $(^7_\Lambda$Li), $(^9_\Lambda$Be), $(^{10}_\Lambda$B), $(^{11}_\Lambda$B), $^{12}_\Lambda$C, $^{13}_\Lambda$C, $^{14}_\Lambda$N, $(^{15}_\Lambda$N), $(^{16}_\Lambda$O), $^{18}_\Lambda$O, $^{19}_\Lambda$F, $^{20}_\Lambda$Ne, $^{23}_\Lambda$Na, $^{27}_\Lambda$Al, and $^{28}_\Lambda$Si. The hypernuclei in parenthesis were already studied with Hyperball in E419, E930 and E518, but most of them have to be investigated again to get complete level schemes or better $B(E2)$ values.

First we run a survey experiment by using a beam time of one or a half day (normalized for the full beam) for each of 1.1 and 0.8 GeV/c and for each target in order to roughly construct a level scheme of each hypernucleus. In the second step, after the survey experiment, we pick up several important or interesting hypernuclei such as $^{12}_\Lambda$C, $^{13}_\Lambda$C, $^{20}_\Lambda$Ne, and $^{28}_\Lambda$Si, and spend a beam time of several days (for full beam) per each in order to assign spin-parities of each level and to construct a complete level scheme.

3.5.1 Example of $^{12}_\Lambda$C

We describe more about the second-step experiment, taking $^{12}_\Lambda$C for example. Here we also demonstrate possibilities and usefulness of hypernuclear γ-ray spectroscopy including $\gamma\gamma$ coincidence, angular correlations, and polarizations. We will reveal the complete level structure of bound states in $^{12}_\Lambda$C and make spin assignments experimentally.
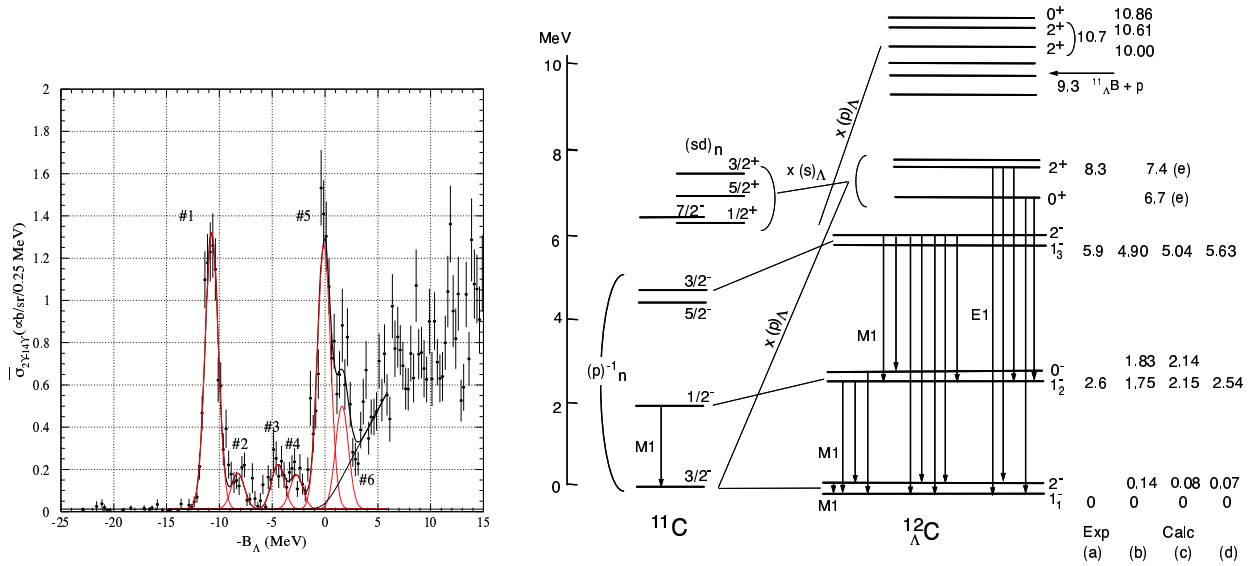

Figure 22: Top: $^{12}_\Lambda$C spectrum measured by the (π^+,K^+) reaction (KEK E369) [21]. The peaks A, B, C, D are interpreted as 1^-_1, 1^-_2, 1^-_3, and 2^+_1 states. Bottom: Level scheme and expected γ transitions of $^{12}_\Lambda$C hypernucleus. (a) shows experimental level energies (E369), and (b), (c), (d), (e) are calculated energies by Itonaga *et al.* [22], Fetisov *et al.* [23], Millener *et al.* [13], and Motoba [24], respectively.

In the case of $^{12}_\Lambda$C, a level at E_x=8.3 MeV, which is barely separated in the recent (π^+,K^+) spectrum (E369) (see Fig. 22 top) [21], is interpreted as a 2^+ state having a ^{11}C($\frac{5}{2}^+$) $\otimes s_\Lambda$

$(d_N \otimes s_\Lambda)$ configuration but with an admixture of $^{11}\mathrm{C}(J^-) \otimes p_\Lambda$ $(p_N^{-1} \otimes p_\Lambda)$ configurations [25], as illustrated in Fig. 22 bottom. A small admixture of $p_N^{-1} \otimes p_\Lambda$ component makes production cross section of this 2^+ state large. Due to such intershell coupling, a few positive parity states around 7 MeV are expected to be populated. Ref. [25] predicts the first 2^+ and 0^+ states to appear at 7.4 and 6.7 MeV. Since they are particle bound (threshold is at 9.3 MeV), we can precisely determine their level energies from their γ transitions.[1] Their level energies contain information on the $p_\Lambda p_N$ interactions. We can also determine their spin-parities, which is essential because various levels with different spin-parities are expected to exist in this excitation energy region.

$^{12}_\Lambda\mathrm{C}$ – **Yield estimate** Figure 23 shows level energies, cross sections, and γ-ray branching ratios assumed in the simulation. The production cross sections of the $^{12}_\Lambda\mathrm{C}$ states (except for the first 2^+ state) were calculated by Itonaga *et al.* for 1.1 GeV/c (K^-,π^-) reaction [22]. The production yield of the 8.1 MeV state, assigned as the first 2^+ state, can be estimated from Fig. 22 (top) and the Itonaga's calculation, since the cross section ratio between the first 2^+ state (8 MeV) and the dominantly-populated 10–11 MeV two 2^+ states should be the same for the (K^-,π^-) and (π^+,K^+) reactions. The energy levels are taken from the experimental values from E369 but the doublet spacing energies are taken from the new parameter set of the spin-dependent interactions by Millener [13]. The branching ratios are takes from Ref.[22] but corrected for the excitation energies described above. The branching ratios from the 6 MeV 2^- state and 2^+ state are calculated assuming weak coupling limit.[2]

In the yield estimation, we assumed the following values:
· K^- beam intensity: 1.9×10^7 /spill(2×10^{14}ppp)
· PS cycle: 3.4 sec
· Target: 10 g/cm^2 / A $\times 6 \times 10^{23}$
· Spectrometer acceptance: $\Omega_{\pi^-} = 0.02$ sr
· Spectrometer tracking efficiency: $\epsilon_{sp} = 0.5$
· Ge detector efficiency in Fig. 21
· Ge detector livetime: $\epsilon_{Ge\ live} = 0.6$
We estimate γ ray yields for 5 days' run as shown in Fig. 23.

Background and Simulation In the hypernuclear γ-ray spectrum (γ spectrum after the hypernuclear bound state region is gated), the continuous background mainly comes from neutrons and π^0 emitted in hypernuclear weak decays, according to our analysis of E419 data. As we found in the E930 analysis, K^- decay in-flight also causes background in the (K^-,π^-) reaction, but after π^0 events are removed with the BGO counters, K^- decay is not a major part of the background. In addition, it can be completely removed by a kinematical cut using momentum and scattering angle of the outgoing particle.

---

[1]The pure $^{11}\mathrm{C}(3/2^-)_{g.s.} \otimes p_\Lambda$ levels without the coupling exist at 10–11 MeV. Although these states have large production cross sections, they are above the particle emission threshold and their level energies cannot be determined from γ transitions.

[2]The 2^+ state was assumed to be coupled only to $^{11}\mathrm{C}(\frac{5}{2}^+)$, and the transition $2^+ \to 1_2^-$ is suppressed because the core transition is $\frac{5}{2}^+ \to \frac{1}{2}^- (M2)$.

Assuming the same continuous background level (γ-ray counts per gated event in the hypernuclear mass spectrum) as in the E419 experiment, we can simulate the spectrum for the $^{12}_\Lambda$C run. Figure 24 shows the simulated data for 5 days' run. Here the different energy dependence of the Ge detector efficiency is taken into account. We will be able to observe almost all the expected γ lines. Figure 25 shows some examples of γ-γ coincidence spectra. Those spectra enable us to completely reconstruct the level scheme as in Fig. 22.
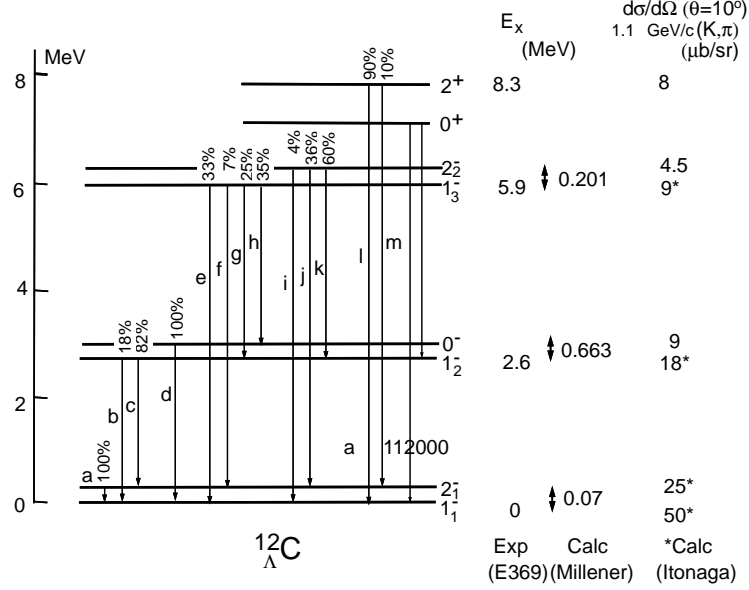

Figure 23: Top: Expected level energies and γ transitions of $^{12}_\Lambda$C used in the simulation. Bottom: Expected yields of γ transitions of $^{12}_\Lambda$C for 5 days' run. Yields of γ-γ coincidence events are also shown.

Angular correlations   When a hypernuclear state with spin J_1 is produced from a target nucleus with J by the (K^-,π^-) reaction with ΔL and ΔS, and then γ-decays into another state with J_2 via Eλ or Mλ transition:

$$^AZ(J) \xrightarrow{(K^-,\pi^-)^{\Delta L,\Delta S}} {}^A_\Lambda Z(J_1) \xrightarrow{\gamma(\lambda)} {}^A_\Lambda Z(J_2),$$
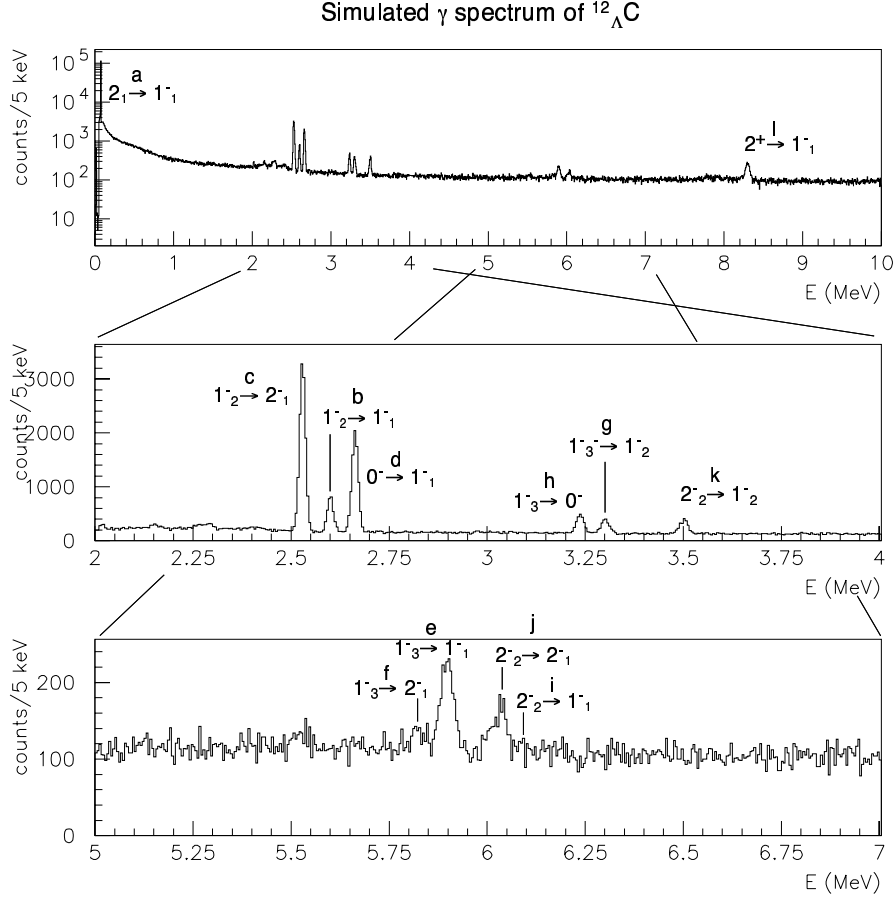
Figure 24: Simulated spectrum of $^{12}_\Lambda$C γ rays for 5 days' run with the (K^-,π^-) reaction at 1.1 GeV/c at the 50 GeV PS. Compton/π^0 suppression and Doppler-shift correction are applied.

the angular correlation exists between π^- and γ, as in the following form for $\Delta S=0$ [3] [8]:

$$W(\theta_{\pi\gamma}) = \sum_{M,M_1,M_2,m} \begin{pmatrix} \Delta L & J & J_1 \\ m & M & M_1 \end{pmatrix}^2 \left[\begin{pmatrix} \lambda & J_2 & J_1 \\ 1 & M_2 & M_1 \end{pmatrix}^2 + \begin{pmatrix} \lambda & J_2 & J_1 \\ -1 & M_2 & M_1 \end{pmatrix}^2 \right] |Y_m^{\Delta L}(\theta_{\pi\gamma})|^2$$

In the case of hypernuclear productions of $\Delta L = 1$, such as productions of low-lying $(p_n^{-1}s_\Lambda)$ levels of p-shell hypernuclei, the equation reduces to a simple from:

$$W(\theta_{\pi\gamma}) \propto 1 + A\cos^2\theta_{\pi\gamma}.$$

This angular correlation is much more sensitive to the spins of the states than the angular correlations between two γ's emitted in a cascade decay. In the case of $^{12}_\Lambda$C, $A = 0$, -1, 1, -1/7 for 0→any, $1^- \to 0^-$, $1^- \to 1^-$, $1^- \to 2^-$ transitions, respectively, and $A = $ -27/53 for the second γ ray in the cascade $1^- \to 2^- \to 1^-$.

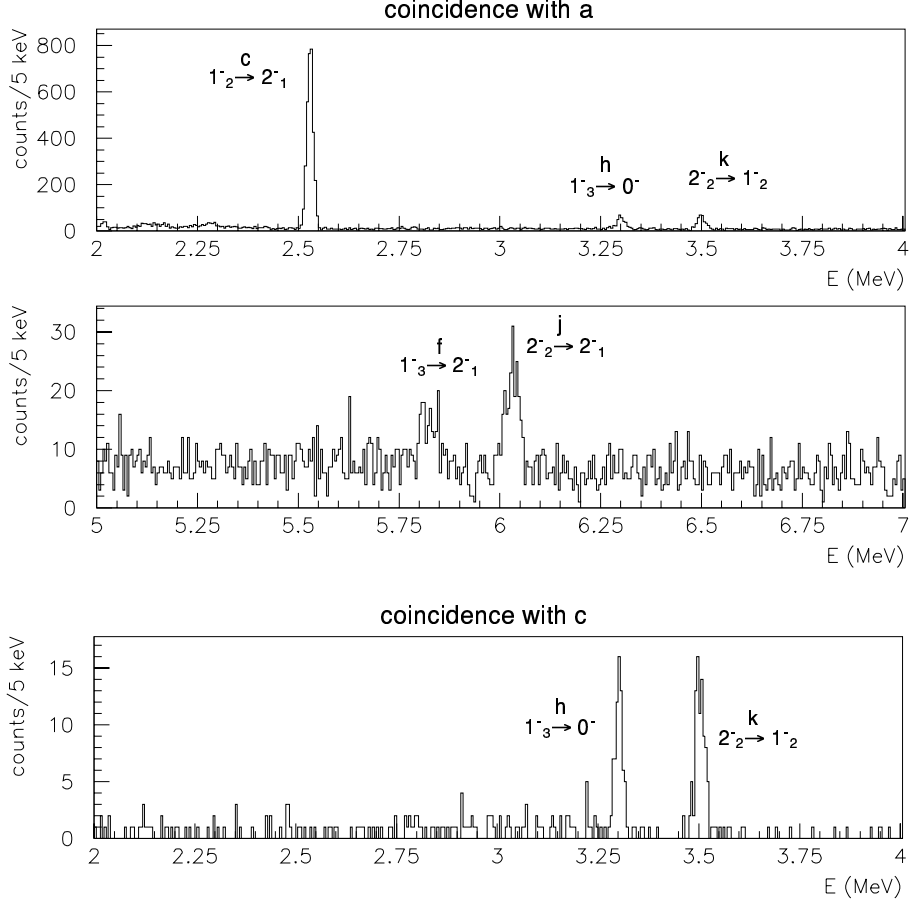[3]The spin-flip case ($\Delta S=1$) is not calculated in Ref.[8].

42

Figure 25: Simulated γ-γ coincidence spectrum of $^{12}_{\Lambda}$C. Top two: coincidence with γ-ray "a" ($1^-_2 \rightarrow 1^-_1$). Bottom: coincidence with γ-ray "c" ($1^-_2 \rightarrow 2^-_1$).

Figure 26 shows simulated $\theta_{\pi\gamma}$ correlations for some of those transitions, indicating that these three types of transitions ($0^- \rightarrow 1^-$, $1^- \rightarrow 1^-$, and $1^- \rightarrow 2^-$) can be clearly discriminated in 5 days' beam time. Combined with level scheme and γ-ray branching ratios, we can completely assign spins of all the bound states of $^{12}_{\Lambda}$C.

3.5.2   Example of $^{20}_{\Lambda}$Ne

In $^{20}_{\Lambda}$Ne we expect an interesting change of cluster structure induced by a Λ. A negative-parity ground state is predicted in $^{20}_{\Lambda}$Ne, being contrary to the naively expected positive parity ground state of $(sd)_n^{-1}(s)_\Lambda$ configuration.

Figure 27 shows expected relevant low-lying levels and transitions of $^{20}_{\Lambda}$Ne. The left part of Fig. 27 is expected from a naive picture, where energies of $(0^+,1^+)$ and 1^- states are taken from a shell-model calculation [9]. The right part shows a result of the cluster model calculation by Sakuda and Bando [26]. Here the negative-parity states of which structure is $^{16}_{\Lambda}$O(p-hole state) + ^{4}He have much lower energies than the 0^+ and 1^+ doublet states having
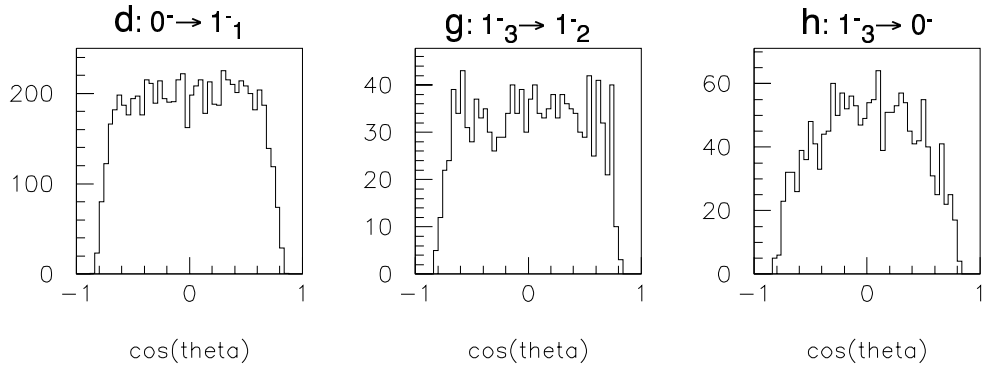
43

Figure 26: Angular distributions between γ and π^- for some $^{12}_{\Lambda}$C transitions (simulated in the same condition as the previous figures).

the ^{16}O + $^{4}_{\Lambda}$He structure. It is because the negative-parity states in ^{19}Ne having a well-clusterized structure of ^{15}O(p-hole state of ^{16}O) + ^{4}He largely shrinks when a Λ is added, while the positive parity states having ^{16}O + ^{3}He structure is not well-clusterized but rather spherical and thus shrinkage by a Λ is expected to be smaller, as illustrated in Fig. 28.

As shown in Fig. 27, expected γ transitions in each case are completely different from each other. In the latter case, the γ transitions stem mainly from the population of the 2^+ state which has a sizable cross section in the (K^-,π^-) reaction. As shown in Fig. 27, the cross section of $^{20}_{\Lambda}$Ne was assumed to be the same as that of $^{18}_{\Lambda}$O, which was calculated for 0.8 GeV/c (K^-,π^-) reaction by Yamada et $al.$[27]. By observing all the transitions shown in Fig. 27 we can reconstruct the level scheme and assign spin parities in the same way as the $^{12}_{\Lambda}$C case, and determine whether the ground state parity is positive or negative.

In addition, the structure of $^{20}_{\Lambda}$Ne, particularly its ground-state doublet, will give us information on the effective ΛN spin-dependent interactions in the sd-shell region, which will then be theoretically discussed in relation to the spin-dependent interactions derived from p-shell hypernuclei.

In the experiment, we use the (K^-,π^-) reaction with 0.8 and 1.1 GeV/c K^- beam from the K1.1 beam line. The yields of γ rays for the 0.8 GeV/c case are estimated as shown in Table 5.

Table 5: Yield estimation of γ transitions of $^{20}_{\Lambda}$Ne for the two cases of level energies predicted by Millener *et al.* [9] and by Sakuda-Bando [26].

Hypernuclei	$^{20}_{\Lambda}$Ne(Millener *et al.*)		$^{20}_{\Lambda}$Ne(Sakuda-Bando)	
Transition	$1^-\to0^+,1^+{}_{gsd}$	$1^+\to0^+$	$2^+\to2^-,1^-_2,1^-_1$	$1^-_2\to1^-_1,0^-{}_{gsd}etc.$
	$E1$	spin-flip $M1$	$E1$	$M1$
γ energy (MeV)	0.70, 0.45	0.25 $^{a)}$	1.72, 1.47, 1.34	0.38, 0.25,..
Reaction used	^{20}Ne$(K^-,\pi^-)^{20}_{\Lambda}$Ne, 0.75 GeV/c $\theta=10^o$			
K^- beam/spill	$2.2\times10^6\ K^-$			
$d\sigma/d\Omega$	200 μb/sr $^{a)}$		45 μb/sr $^{b)}$	
γ branch	0.65, 0.35	0.35	??	??
Target($\times6\times10^{23}$)	10 g/cm^2 / 20			
Spectrometer acceptance	0.02 sr			
Tracking efficiency	0.5			
Ge eff. ($\Omega\times\varepsilon_{peak}$)	17% , 21%	27%	12%	$\sim$20%
Ge livetime (ε_{ele})	0.6			
	$\times60\times60/3.4$ spills$\times24$ hours			
Yield/24 hours	2800, 1900	2400	650 ($E1$ total)	??

$^{a)}$ Estimated by Millener *et al.* [9]
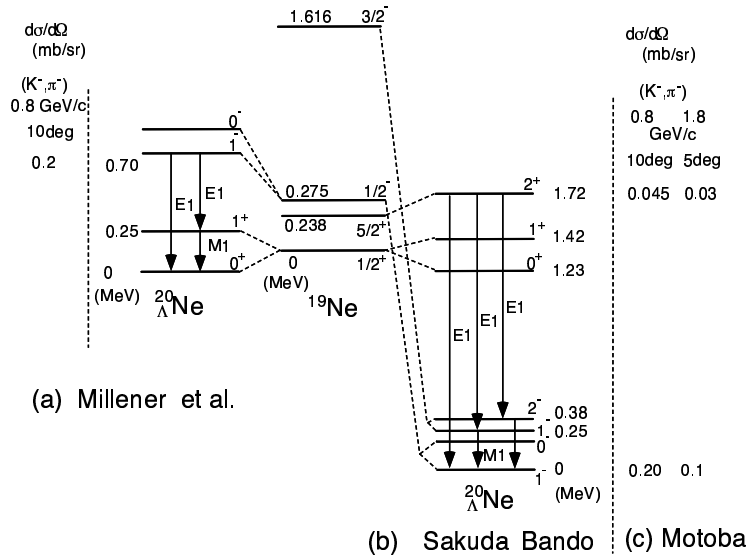$^{b)}$ Estimated by Motoba *et al.* [24].

45

Figure 27: Level scheme and transitions of $^{20}_{\Lambda}$Ne. The expected level scheme and the cross section are calculated by Millener *et al.* with the shell model (left part) [9] and with the cluster model by Sakuda and Bando (right part) [26]. (c) shows estimated cross sections by Motoba [24] from calculated $^{18}_{\Lambda}$O cross sections by Yamada *et al.* [27].
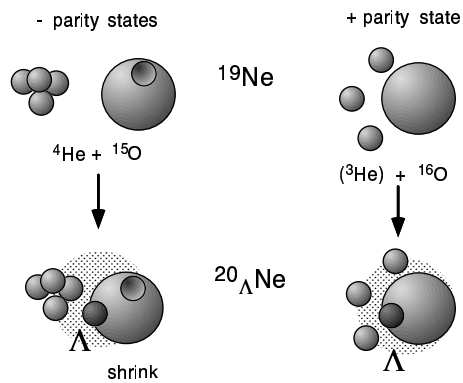

Figure 28: Cluster-model prediction of shrinking effect of $^{20}_{\Lambda}$Ne. When a Λ is added, the negative-parity states having the α-^{15}O cluster structure shrink more than the positive-parity states having a compact (shell-like) structure.

46

3.6 γ Spectroscopy of Medium and Heavy Hypernuclei with (K^-,π^-) Reaction (2)

In medium and heavy hypernuclei, level energies of p_Λ states provide information on the odd-state ΛN interactions as described in Sect. 3.2.1. We plan γ spectroscopy of several hypernuclei such as $^{89}_\Lambda$Y, $^{139}_\Lambda$La, and $^{208}_\Lambda$Pb, where we will detect $p_\Lambda \to s_\Lambda$ $E1$ transitions and other transitions in coincidence with the $E1$ transitions. In order to give a large momentum transfer to populate deeply bound p_Λ states, we had better use 1.8 GeV/c (K^-,π^-) reaction at large scattering angles at K1.8 beam line. We require a beam time of a few days (for full beam) per each hypernucleus. The $^{89}_\Lambda$Y experiment is also going to be proposed at BNL AGS [28].

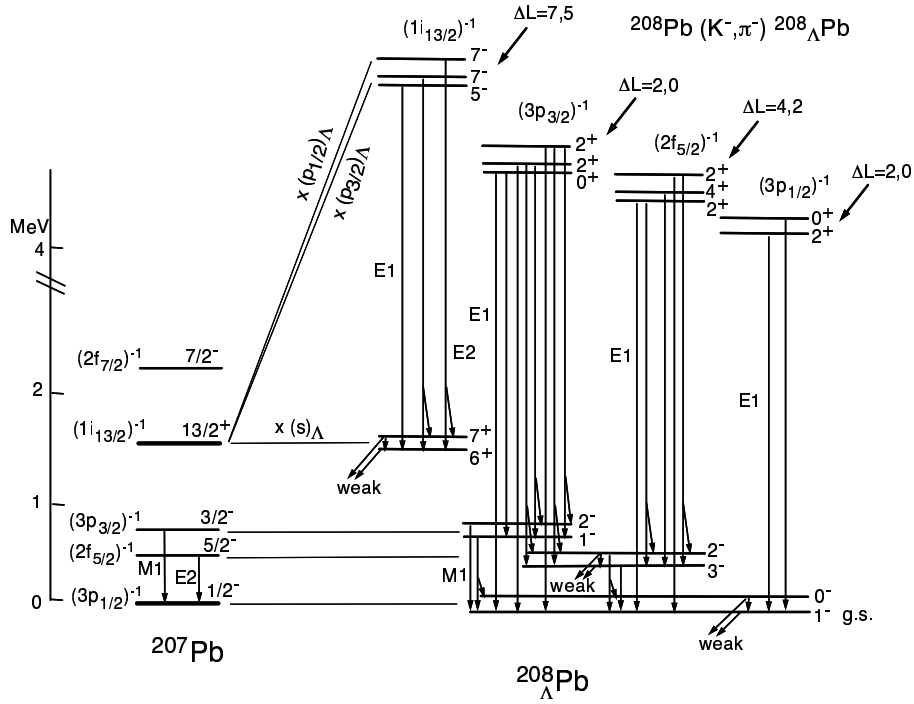Figure 29: Expected level scheme and γ transitions of $^{208}_\Lambda$Pb. Only non-spin-flip states are shown for the p_Λ states.

3.6.1 Example of $^{208}_\Lambda$Pb

In $^{208}_\Lambda$Pb, the excitation energy of the p_Λ states was measured to be 4.5±0.6 MeV [29], being smaller than the proton/neutron separation energy of 6.7 MeV. Figure 29 shows expected low-lying level scheme and γ transitions of $^{208}_\Lambda$Pb. Here we assume one-hole configurations for ^{207}Pb core and weak coupling between a Λ and the core. γ transitions are characterized by many 4–5 MeV $E1(p_\Lambda \to s_\Lambda)$ transitions, some of which are followed by $M1$ or $E2$ core transitions.

We estimate γ-ray yields for $^{208}_\Lambda$Pb. We use the reaction ^{208}Pb$(K^-,\pi^-)^{208}_\Lambda$Pb at 1.8

GeV/c to efficiency populate p_Λ states coupled to the $i_{13/2}$ hole state (1633 keV isomer of ^{207}Pb). There are three possible non-spin-flip $n \to \Lambda$ transitions, namely $i_{13/2} \to p_{1/2}$ and $i_{13/2} \to p_{3/2}$ with $\Delta L = 7$ and $i_{13/2} \to p_{3/2}$ with $\Delta L = 5$ (see Fig. 29). The cross sections of those states were calculated as shown in Fig. 30 [30].

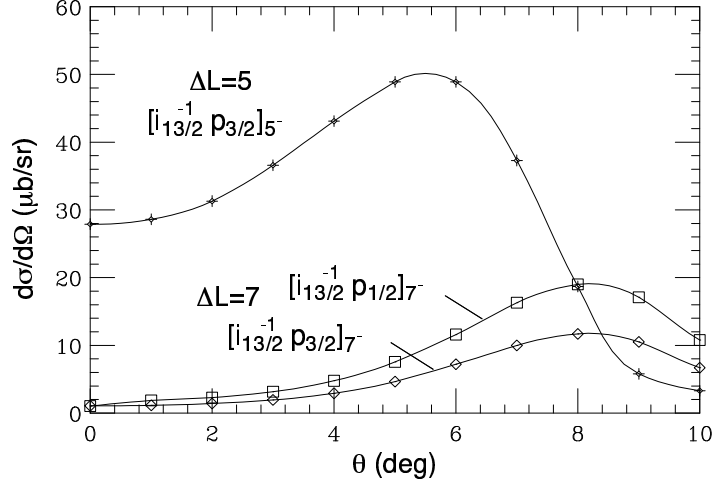Figure 30: Calculated cross sections for the $\Delta L = 7$ transitions and for the $\Delta L = 5$ transition in the 1.8 GeV/c (K^-,π^-) reaction [30].

Those populated states, $[(1i_{13/2})_n^{-1}(1p_{1/2})_\Lambda]_{7^-}$ $[(1i_{13/2})_n^{-1}(1p_{3/2})_\Lambda]_{7^-,5^-}$, undergo 4 MeV $E1(1p_\Lambda \to 1s_\Lambda)$ transitions to the doublet $(7^+,6^+)$. By assuming the same K^- intensity and the other conditions as in the $^{12}_\Lambda$C case, the expected yields for those transitions are obtained as 3000, 1800, and 6800 events, respectively, for a beam time of 24 hours.

In the same way, other p_Λ states coupled to other hole states, $(3p_{1/2})_n^{-1}$, $(2f_{1/2})_n^{-1}$, and $(3p_{1/2})_n^{-1}$, corresponding to the ground, 570 keV, and 898 keV states of ^{207}Pb, can also be populated, and their $E1(p_\Lambda \to s_\Lambda)$ transitions can be observed (see Fig. 29). Since the production cross sections of different hole states are sensitive to the momentum transfer, we can identify initial states of γ transitions from π^--angular dependence of those γ-ray yields and/or using different (lower) incident K^- momenta.

3.7 γ Spectroscopy of Hyperfragments (3)

In direct reactions, such as (K^-, π^-), hypernuclear species that can be studied are limited by target availability. On the other hand, it is known that various hypernuclei, including proton or neutron rich ones, can be produced as hyperfragments by K^- induced reactions. Therefore, the use of hyperfragments further extends the possibility of hypernuclear γ-ray measurements.

We are considering two ways to produce hyperfragments, K^--in-beam method and stopped K^- method.

K^--in-beam method   One is to use inclusive (K^-, π) reactions at $P_{K^-} = 0.8$–1.1 GeV/c. In this momentum range, recoil momentum of Λ in the elementary processes are comparable to or smaller than Fermi momentum of Λ in hypernucleus, and thus the chance that the produced Λ is trapped to form a hypernucleus is quite large.

The experimental setup is similar to that used for the direct (K^-, π^-) reaction described in Sect. 3.5. The only difference is that while medium to high resolution spectrometer is required for direct reaction based experiments to identify production of bound states of a hypernucleus, we need little or no information on momenta of incoming K^- and outgoing π^- to detect γ rays from hyperfragments. Thus we have broad choice on the experimental setup; we can share the same setup as that described in Sect. 3.5 and run parasitically, or use inexpensive, poor-resolution spectrometer such as KURAMA or TOKIWA, in case high-resolution spectrometer is not available due to budgetary limitation.

An initial trial was performed at BNL-AGS E930 in 2001, where ^{10}B(K^-, π^-) reaction at 0.93 GeV/c was used. With a beam time of as short as 48 hours, we observed several γ rays from hyperfragments such as $^{7}_{\Lambda}$Li and $^{9}_{\Lambda}$Be, as shown in Fig. 31 (a), when the slightly unbound mass region is roughly selected. Furthermore, the 2050 keV $^{7}_{\Lambda}$Li γ ray was clearly seen even without using the momentum information of incoming K^- and outgoing π^-, as shown in Fig. 31 (b). In this experiment, it was shown that identification of kaons and pions can be done with Cherenkov counters only with good purity. At JHF, considering the higher beam intensity and improved detection efficiency of upgraded Hyperball, we can accumulate the same amount of data in a few hours.

Thus, it is rather easy to observe γ rays from hyperfragments. In order to identify observed γ rays, γ-γ coincidence measurement is essential. It was also demonstrated even in E930 with the un-upgraded (small-efficiency) Hyperball; as shown in Fig. 31 (c), we succeeded in observing a peak for $^{7}_{\Lambda}$Li$(7/2^+ \rightarrow 5/2^+)$ transition at 470 keV, by taking γ rays emitted in coincidence with the 2050 keV $5/2^+ \rightarrow 1/2^+$ transition. At the 50 GeV PS, the use of more intense K^- beam and the upgraded Hyperball makes such coincidence measurements easier.

Stopped K^- method   The other method is to use stopped K^-, which is useful at a very initial stage where intensity of primary proton is low. In this method, kaons are degraded, stopped in the target, and absorbed by a nucleus to produce a hyperon very efficiently. It is known from emulsion experiments that about 10% of kaons stopped on light nuclear targets (A=12-16) make hypernuclei as hyperfragments [31]. This is the most efficient way to produce
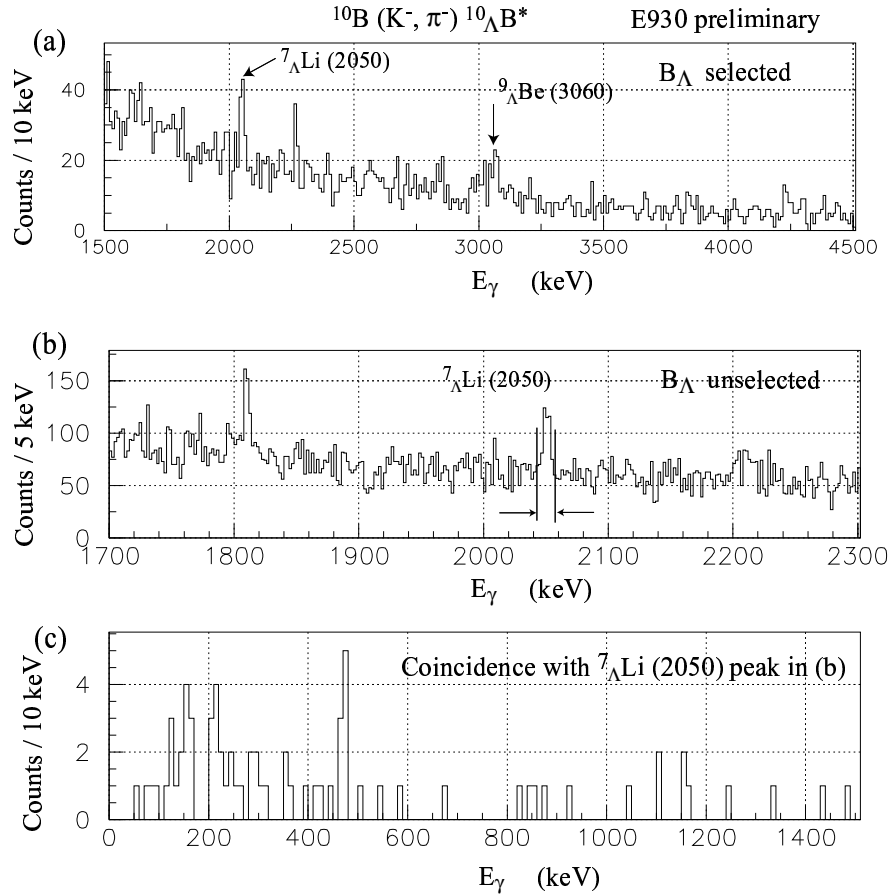
Figure 31: Preliminary γ-ray energy spectra for ^{10}B$(K^-, \pi^- \gamma)$ reaction obtained in BNL E930. (a) Missing mass of $^{10}_\Lambda$B was selected for $-10 < -B_\Lambda < 30$ MeV. γ rays from $^7_\Lambda$Li and $^9_\Lambda$Be are observed. (b) No selection on the missing mass of $^{10}_\Lambda$B was applied. The $^7_\Lambda$Li γ ray peak is still prominent. (c) Spectrum of γ rays which coincide with the 2050 keV $^7_\Lambda$Li $(5/2^+ \to 1/2^+)$ γ ray in (b) gated for 2043 keV $< E_\gamma <$ 2057 keV. A peak at 470 keV is seen clearly, and is assigned as the $^7_\Lambda$Li$(7/2^+ \to 5/2^+)$ transition.
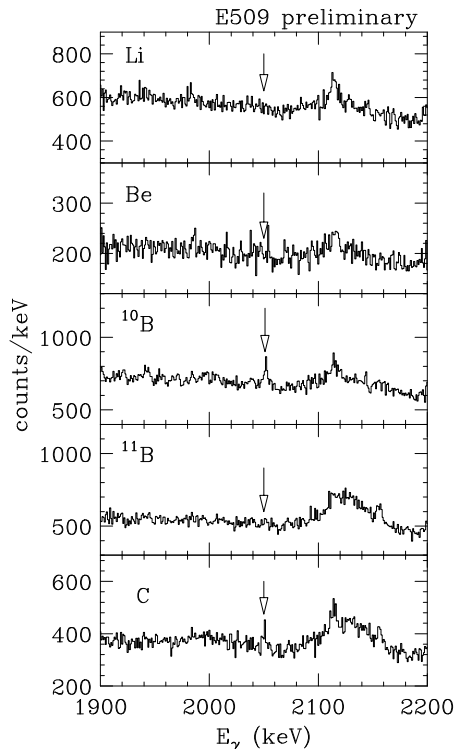
Figure 32: Preliminary γ-ray energy spectra from stopped K^- absorption on Li, Be, ^{10}B, ^{11}B, and C targets obtained in KEK E509. The 2050 keV γ ray from $^7_\Lambda$Li($5/2^+ \to 1/2^+$) is observed for ^{10}B and C targets.

hypernuclei, although the background level is also high. γ-γ coincidence measurement as well as target dependence of γ-ray yields enable us to identify hypernuclear species.

Recently, a pioneering experiment (E509) was conducted at the K5 beam line at KEK using 0.6 GeV/c K^- degraded and stopped in several light nuclear targets [5]. In a short beam time, we observed 2050 keV $^7_\Lambda$Li γ ray in ^{10}B and ^{12}C targets (see Fig. 32), in addition to a few unassigned hypernuclear γ rays. The yield of the $^7_\Lambda$Li γ ray is about 1.5×10^{-3} per stopped K^-.

According to the Sanford-Wang formula, we can expect 2.5×10^4 negative kaons of 0.6 GeV/c at the K1.1 line for 2×10^{13} 30 GeV protons (about 1/10 of the number of protons delivered in a spill for full intensity) per spill. Assuming 20% for kaon stopping efficiency, we expect 4×10^8 stopped kaons in 3 days of beam time. If we assume a typical γ-ray intensity is of the order of 0.1% per stopped K^-, we can observe peaks of some several 10^4 counts of γ rays in singles measurement with the upgraded Hyperball in 3 days. Even for γ-γ coincidence measurements, peaks with $\sim 10^3$ counts, which allows us to measure angular correlation, are expected.

Plans At the 50 GeV PS, we plan systematic study of hyperfragment γ spectroscopy with all possible p-shell target nuclei (^{7}Li, ^{9}Be, ^{10}B, ^{11}B, ^{12}C, ^{13}C, ^{14}N, and ^{16}O) with the K^--in-

beam method or the stopped K^- method, either of which is chosen depending on available K^- beam intensity and quality. We use a beam time of a few days per target and search for various hypernuclear γ rays, particularly from $A = 8$ hypernuclei and neutron-rich/proton-rich hypernuclei which cannot be accessed by the direct (K^-,π^-) and (K^-,π^0) reactions.

3.8 γ Spectroscopy with (K^-,π^0) Reaction (4)

By using the (K^-,π^0) reaction which converts a proton into a Λ, we can produce some neutron-rich hypernuclei, and mirror hypernuclei of those produced by (K^-,π^-) and (π^+,K^+) reactions. A Λ implanted in a neutron-rich nucleus having a neutron skin or halo may result in a drastic change of the nuclear structure, such as disappearance of neutron skin/halo and large shrinkage. From this viewpoint, measurements of level scheme and $B(E2)$ of n-rich hypernuclei such as $^7_\Lambda$He, $^9_\Lambda$Li, and $^{11}_\Lambda$Be produced by (K^-,π^0) reaction on ^{7}Li, ^{9}Be, and ^{11}B targets are particularly interesting.

The study of charge symmetry breaking in ΛN interaction can be studied by precise comparison of level structure between mirror hypernuclei, such as $^4_\Lambda$H - $^4_\Lambda$He, $^{12}_\Lambda$B - $^{12}_\Lambda$C, $^{16}_\Lambda$N - $^{16}_\Lambda$O, *etc.* Here $^4_\Lambda$H, $^{12}_\Lambda$B, and $^{16}_\Lambda$N are produced by the (K^-,π^0) reaction on ^{4}He, ^{12}C, and ^{16}O targets.

In the experiment, we use both of 1.1 and 0.8 GeV/c K^- beam. We require beam time of roughly 10+10 days (for full beam) for each target.

3.8.1 Example of $^7_\Lambda$He

^{6}He is a neutron-rich nucleus having a two-neutron skin. The first excited state of 2^+ is observed as an unbound resonance state (see Fig. 33), but its structure is not well known; the $B(E2; 2^+\rightarrow0^+)$ has not been experimentally obtained.

Figure 33 shows the expected level scheme and the density distribution of valence neutrons of ^{6}He and $^7_\Lambda$He calculated by Hiyama with a cluster model for $\alpha + n + n$ and $^5_\Lambda$He $+n+n$ [32, 33]. When we add a Λ to ^{6}He, the neutron skin in the ground state is expected to shrink. The ^{6}He(2^+) state, which has widely-spread two valence neutrons, becomes bound by a Λ, and the core $E2$ transitions ($\frac{5}{2}^+,\frac{3}{2}^+\rightarrow\frac{1}{2}^+$) are observed. The $B(E2)$ of ^{6}He($2^+ \rightarrow 0^+$) is calculated to be 0.58 e^2fm^4, while the corresponding $B(E2)$ of $^7_\Lambda$He is calculated to be 0.068 and 0.059 e^2fm^4 for $\frac{5}{2}^+\rightarrow\frac{1}{2}^+$ and $\frac{3}{2}^+\rightarrow\frac{1}{2}^+$, respectively [33]. The predicted change of $B(E2)$ is caused by a drastic shrinkage of valence neutron wavefunctions in ^{6}He induced by a Λ, as shown in Fig. 33.

In the present case, these $E2$ transitions are competing against weak decay. If we assume the weak decay rate of these states to be $(200 \text{ ps})^{-1}$, then it is expected that the lifetimes of these states are 140 ps and 170 ps, and that the branching ratios for the $E2$ γ transitions are 42% and 17%. We will directly measure the lifetimes of these excited states with weak-decay particles (π^- and proton). Combined with the branching ratios of those $E2$ transitions, the $B(E2)$'s can be derived.

In the $^7_\Lambda$He experiment, we use the ^{7}Li(K^-,π^0) reaction with 0.8 GeV/c K^- beam from the K1.1 beam line and employ a high-resolution π^0 spectrometer. In order to separately identify production peaks for the $\frac{5}{2}^++\frac{3}{2}^+$ states and the $\frac{1}{2}^+$ states which are expected to

be 1.7 MeV apart from each other, the π^0 spectrometer should have a resolution better than 2 MeV FWHM. In order to measure the lifetime of the excited states with weak-decay particles, we install the "decay arm" counter system which consists of fast plastic counters and a stack of plastic counters, as described in Fig. 35.

The yields of weak-decay particles and γ rays are estimated by assuming the following conditions.

· K^- beam intensity: 2.2×10^6 /spill(2×10^{14}ppp)
· PS cycle: 3.4 sec
· Target: 10 g/cm^2 /7 $\times 6 \times 10^{23}$
· Cross section: $d\sigma/d\Omega(\frac{5}{2}^+, T=1) \sim 25$ μb/sr at 10^0
· Branching ratio for $E2$ γ ray: 42% [4]
· Spectrometer acceptance: $\Omega_{\pi^0} = 0.01$ sr
· Spectrometer tracking efficiency: $\epsilon_{sp} = 0.4$
· Ge detector efficiency : $\epsilon(\text{Ge}) = 0.09/2$ at 1.7 MeV
· Ge detector livetime: $\epsilon_{Ge~live} = 0.6$
· Efficiency for weak decay particle: $\epsilon_{weak} = 0.1$

We expect 1700 events for weak decay particles and 330 events for the $E2$ γ rays in a beam time of 10 days. Statistical accuracy for $B(E2)$ will be less than 10%, although it may have a systematic error from decomposition of the $\frac{5}{2}^+(T=1)$ peak from the $\frac{1}{2}^+(T=1)$ peak in the (K^-, π^0) spectrum. The resolution of the π^0 spectrometer is a key issue.

---

[4]Roughly estimated from calculated $\Delta L=1$ states of $^{12}_{\Lambda}$C at 0.8 GeV/c and calculated $^{12}_{\Lambda}$C and $^{7}_{\Lambda}$Li states at different conditions [22, 24].
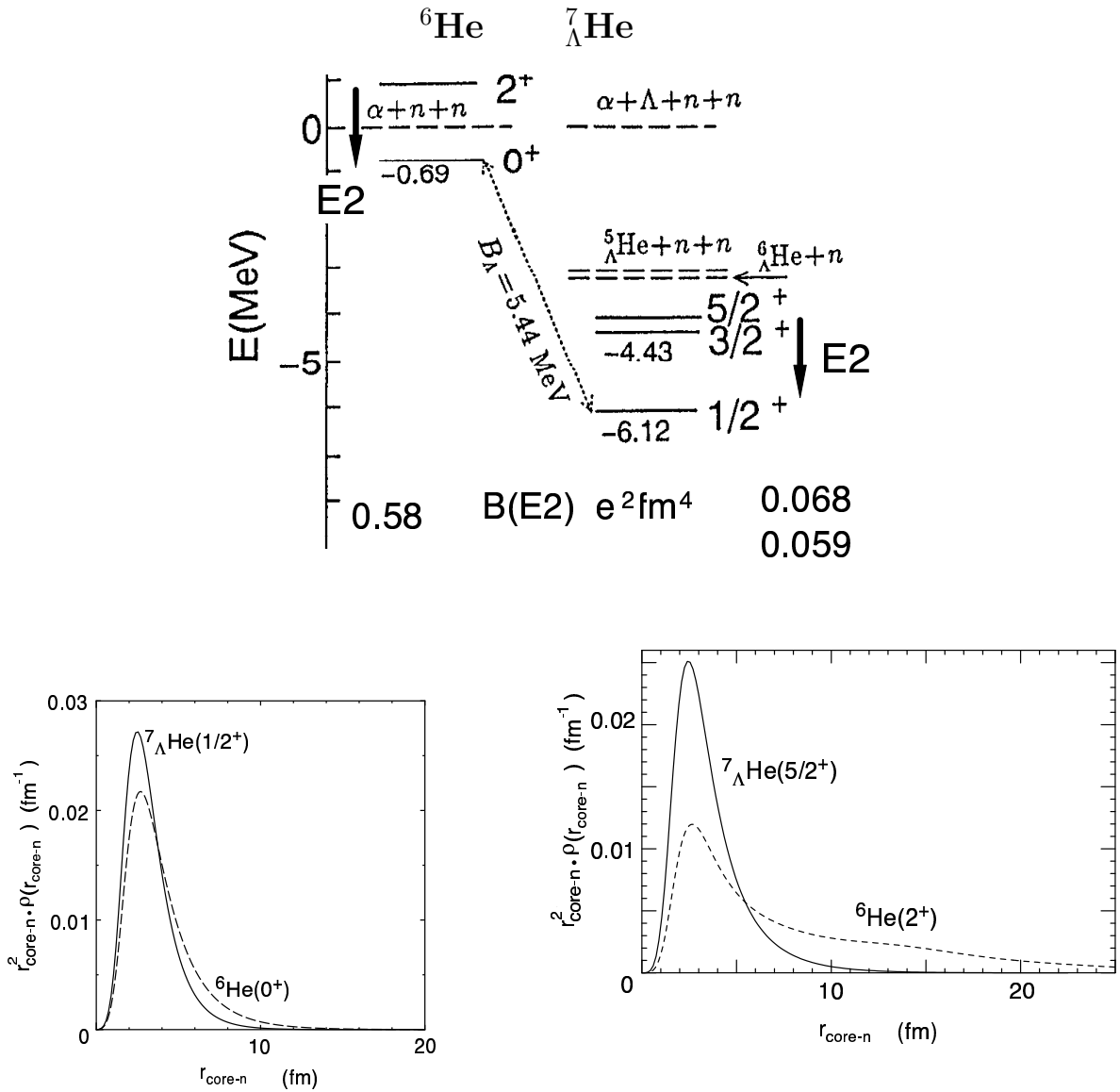
Figure 33: Top: Expected level scheme of $^{7}_{\Lambda}$He and $B(E2)$ calculated by Hiyama *et al.* with a 3-body (α ($^{5}_{\Lambda}$He) $+n+n$) cluster model [32]. Bottom: Calculated density distribution of valence neutrons are compared for ^{6}He(0^{+}) and $^{7}_{\Lambda}$He($\frac{1}{2}^{+}$), and for ^{6}He(2^{+}) and $^{7}_{\Lambda}$He($\frac{5}{2}^{+}$) [33].

3.9 $B(M1)$ **Measurements with Doppler Shift Attenuation Method (5)**

At 50 GeV PS, we plan to measure reduced transition probabilities $B(M1)$ for spin-flip $M1$ transitions of various hypernuclei, for the purpose of studying Λ g-factor in various nuclei. In general, in order to measure γ-transition probabilities such as $B(M1)$ and $B(E2)$, we need to know a lifetime of the excited state which undergoes the transition. If the excited state also has other decay branches such as weak decay or other γ transitions, we also need to measure the branching ratio of the particular transition.

We proposal two different methods of the $B(M1)/B(E2)$ measurement depending on the lifetime of the upper state. When the lifetime is $10^{-12} \sim 10^{-11}$ sec, Doppler-shift attenuation method (DSAM) is used to measure the lifetime. When it is comparable to the weak decay lifetime of Λ ($\sim 10^{-10}$ sec), we propose to use the "γ-weak coincidence" method described in the following section. In the former case, we need to choose the optimum reaction (velocity of recoil hypernucleus) and the target density so that the lifetime of the excited state and the stopping time in the target shall be comparable. The γ-ray peak shape which is partly-broadened by Doppler shift gives lifetime of the state, as we did in the $B(E2)$ measurement of $^{7}_{\Lambda}$Li in E419 [3].

Recently we carried out an experiment at KEK (E518) for the purpose of measuring $B(M1)$ of $^{11}_{\Lambda}$B, where the spin-flip $M1$ transition of $^{11}_{\Lambda}$B($3/2^+ \to 1/2^+$) is expected to have a lifetime suitable to measure by DSAM [34]. Several γ rays of $^{11}_{\Lambda}$B have already been observed, and the $B(M1)$ value will be able to be measured after full analysis of the data. However, the statistics seems insufficient to precisely determine $B(M1)$ and discuss a possible change of g_Λ in a nucleus.

In the 50 GeV PS, we will continue the E518 experiment to increase the statistics to get a g_Λ value within 5% error. In this experiment we use the (π^+,K^+) reaction with the highest intensity that our detectors can accept (about 10^7 pions/sec). With the fully upgraded Hyperball, we need about 20 days beam time. Since the necessary proton intensity is only 3×10^{12}/sec, this experiment should be done in a very early stage of the machine commissioning.

Then we plan another experiment to measure $B(M1)$ of $^{7}_{\Lambda}$Li($3/2^+ \to 1/2^+$), which is a similar transition as the $^{11}_{\Lambda}$B case. It provides consistency check with the g_Λ value from $^{11}_{\Lambda}$B. It requires the (K^-,π^-) reaction with high intensity 1.1 GeV/c beam to directly populate the spin-flip $3/2^+$ state. In order to adjust the recoil velocity, we use a Li-Pb alloy target. We need a beam time of about 5 days (normalized for the full beam).

Depending on the results of $^{11}_{\Lambda}$B/$^{7}_{\Lambda}$Li data and level scheme of various hypernuclei determined from experiments (1) and (2), we will be able to find other good candidates to measure $B(M1)$. In order to see the effect of $B(M1)$ change due to meson exchange current of two-pion exchange in the $\Sigma - \Lambda$ coupling, $B(M1)$ measurement of states with non-zero isospin is important.

3.10 $B(M1)$ **Measurements with γ-Weak Coincidence Method (6)**

When the lifetime of the γ-ray emitting state is comparable to the weak decay lifetime of Λ ($\sim 10^{-10}$ sec), it can be measured by a new method named "γ-weak coincidence method". In

particular, this method is applicable to $B(M1)$ measurement of medium and heavy hypernuclei which usually have small (< 0.1 MeV) double spacings. With this method, we plan to measure $B(M1)$ for several hypernuclei ranging from light to heavy hypernuclei so that we may be able to see nuclear-density dependence of Λ g-factor. Since it is a high-statistical triple-coincidence experiment, we need a long beam time of a few weeks per target with the full beam intensity.

3.10.1 γ-Weak Coincidence Method

As explained in Fig. 34, we measure the lifetime of the upper state B directly from the time difference of hypernucleus production and the emission of weak decay particles (protons and π^-) in coincidence with γ transitions of $B{\to}A$. The branching ratio m of the $B{\to}A$ transition is measured from the γ-ray yield of $B{\to}A$ in coincidence with the $C{\to}B$ transition. If there are no γ transitions like $C{\to}B$ from upper state, we need to separate B and A in the (K^-,π) spectrum, which is usually impossible for the doublet states of (A, B).

The time spectrum of weak-decay particles measured in coincidence with the $B{\to}A$ γ ray is expressed as:
$$P^{B\to A}(t) = \frac{\lambda_A \lambda_B}{\lambda_B - \lambda_A} m N_B^0 (e^{-\lambda_A t} - e^{-\lambda_B t}),$$
where λ_B and λ_A denote the total decay rates of B and A, and N_B^0 denotes the initial population of the state B. From this growth-decay function, we can determine λ_B and λ_A.

When the $B{\to}A$ γ transition is much slower than the weak decay and this transition is suppressed, the number of γ-weak coincidence events decreases, which makes the sensitivity for λ_B worse. In such a case, however, λ_B can be determined from the time spectrum of weak-decay particles in coincidence with the $C{\to}B$ γ rays, which is approximately a single exponential decay with λ_B. In general, the time spectrum measured in coincidence with the $C{\to}B$ γ ray is:

$$P^{C\to B}(t) = \lambda_B N_B^0 [(1 - m\frac{\lambda_B}{\lambda_B - \lambda_A})e^{-\lambda_B t} + m\frac{\lambda_A}{\lambda_B - \lambda_A}e^{-\lambda_A t}].$$

By measuring both of $P^{B\to A}(t)$ and $P^{C\to B}(t)$ and fitting them together to the equations above, we can precisely determine λ_B for a wide range of λ_B. The sensitivity of the $B(M1)$ measurement is discussed in the following sections.

3.10.2 Setup for γ-Weak Coincidence Method

The setup for the γ-weak coincidence measurement is shown in Fig. 35. A half of the Ge detectors in Fig. 20 are replaced by two sets of "decay arm" similar to those used in our previous experiment of hypernuclear lifetime measurement (KEK E307) [35]. The solid angle for the decay particles is about 30% of 4π sr.

Just upstream of the target we install fine-segmented fast plastic scintillation counters which give start-timing signals. In the decay arm, fast scintillators for stop-timing signals are installed as close as possible to the target, and then the fine-segmented SSD is installed to track the decay particles. Behind them are a stack of scintillation counters for dE/dx and

range measurements. Protons and pions are identified and their velocities are measured from the range, dE/dx, and TOF information. According to our previous experience (E307), we can achieve 200 ps FWHM as the overall time resolution of the timing counters. Considering the emission rate of energetic protons or π^- used for lifetime measurement, the efficiency for weak-decay particles will be about 10%.

3.10.3 Expected Results – $^{12}_{\Lambda}$C Case

Here we consider the case of $^{12}_{\Lambda}$C for example. According to the Millener's latest calculation with the new parameter set of the ΛN spin-dependent interactions from our E419/E930 results, the ground-state doublet spacing of $^{12}_{\Lambda}$C is predicted to be 0.071 MeV. The $B(M1)$ of this transition is predicted to be 0.44 μ_N^2 [8], which corresponds to the decay rate of (360 ps)$^{-1}$ for 0.071 MeV. By assuming that the weak decay rate of the upper (2^-) state is the same as that of the ground (1^-) state, (228 ps)$^{-1}$, we estimate the branching ratio of the γ transition to be m=0.39.

We use 1.1 GeV/c (K^-, π^-) reaction to effectively populate the 2^- state. We assume the same beam/spectrometer conditions and use the cross sections and γ-ray branching ratios in Fig. 23. We also assume the following conditions:

· K^- beam intensity: 1.9×10^7 /spill(2×10^{14}ppp)
· PS cycle: 3.4 sec
· Target: 10 g/cm^2 / A $\times 6 \times 10^{23}$
· Cross section $\times$ branching ratio: $d\sigma/d\Omega(1^-)_{total} = 47 \mu$b/sr at 10^0
· Spectrometer acceptance: $\Omega_{\pi^-} = 0.02$ sr
· Spectrometer tracking efficiency: $\epsilon_{sp} = 0.5$
· Ge detector efficiency : $\epsilon(\text{Ge}) = 0.10$ at 0.071 MeV
· Ge detector livetime: $\epsilon_{Ge\ live} = 0.6$
· Efficiency for weak decay particle: $\epsilon_{weak} = 0.1$

Then we expect 15000 γ-weak coincidence events in 400 hours run for m=1. Here, those events in which the 2^- state is populated via γ-ray cascade from other excited states are included, because all those preceding transitions are $M1$ or $E1$ with high energies (> 2 MeV), being thus much faster than the 0.7 MeV spin-flip $M1$ transition, and does not affect the time distribution of the weak decay after the spin-flip $M1$ transition.

In order to estimate accuracy of the $B(M1)$ measurement, we made a simulation of λ_B measurement for the case of $^{12}_{\Lambda}$C. Figure 36 shows simulated time spectra of the weak-decay particles in coincidence with the spin-flip $M1(2^- \rightarrow 1^-)$ transition and in coincidence with the upper $1^-_2 \rightarrow 2^-$ transition, for various cases of the spin-flip transition rate. Figure 37 shows sensitivity of $B(M1)$ determination in the present conditions. Only statistical errors are included. The beam time of 400 hours allows us to measure the $B(M1)$ within 5% statistical error for a wide range of $B(M1) = 0.1$–10 μ_N. Although there may exist systematic errors of ~5% in the branching ratio (m) and the lifetime (λ_B), we can determine $B(M1)$ within 10% error in total.

References

[1] H. Tamura, Nucl. Phys. **A639** (1998) 83c.

[2] H. Tamura *et al.*, Phys. Rev. Lett. **84**, 5963 (2000).

[3] K. Tanida *et al.*, Phys. Rev. Lett. **86**, 1982 (2001).

[4] H. Akikawa *et al*, Phys. Rev. Lett. **88**, 082501 (2002).

[5] K. Tanida *et al.*, Proc. Int. Conf. on Particles and Nuclei (PANIC02), Osaka, September-October 2002, Nuclear Physics A, in press.

[6] H. Tamura *et al.*, Proc. 2nd Asia Pacific Conf. on Few-Body Problems in Physics, Shanghai, August 2002, Modern Physics Letter A, in press.

[7] S. Ajimura *et al.*, Phys. Rev. Lett. **86** (2001) 4255.

[8] R.H. Dalitz and A. Gal, Ann. Phys. **116** (1978) 167; J. Phys. G 6 (1978) 889.

[9] D.J. Millener, A. Gal, C.B. Dover, R.H. Dalitz, Phys. Rev. **C 31** (1985) 499.

[10] Y. Akaishi *et al.*, Phys. Rev. Lett. **84** (2000) 3539.

[11] A.R. Bodmar and Q.N. Usmani, Phys. Rev. **C 31** (1985) 1400.

[12] Y. Yamamoto, S. Nishizaki, and T. Takatsuka, Nucl. Phys. **A 691** (2001) 432c.

[13] D.J. Millener, Nucl. Phys. **A 691** (2001) 93c.

[14] T. Motoba, H. Bandō and K. Ikeda, Prog. Theor. Phys. **80** (1983) 189.

[15] E. Hiyama, M. Kamimura, K. Miyazaki and T. Motoba, Phys. Rev. **C 59** (1999) 2351.

[16] H. Tamura, Eur. Phys. J. **A 13** (2002) 181.

[17] E.V. Hungerford and L.C. Biedenharn, Phys. Lett. **142B** (1984) 232; T. Yamazaki, *Nucl. Phys.* **A 446** (1985) 467c.

[18] T. Takeuchi, K. Shimizu, K.Yazak, Nucl. Phys. **A 481** (1988) 693.

[19] K. Saito, M. Oka, T. Suzuki, Nucl. Phys. **A 625** (1997) 95; M. Oka, K. Saito, K. Sasaki, T. Inoue, *"Hadrons and Nuclei"* ed. Il-T. Cheon *et al.*, American Institute of Physics (2001) p.163.

[20] A. Rusek, Nucl. Phys. A639 (1998) 111c; R.L. Gill, Nucl. Phys. A691 (2001) 180c.

[21] H. Hotchi *et al.*, Phys. Rev. **C 64** (2001) 044302.

[22] K. Itonaga *et al.*, Prog. Theor. Phys. Suppl. **117** (1994) 17.

[23] V.N. Fetisov, L. Majling, J. Žofka and R.A. Eramzhyan, Z. Phys. **A 339** (1991) 399.

[24] T. Motoba, private communication (1995,1996,1999).

[25] T. Motoba, Nucl. Phys. **A639** (1998) 135c.

[26] T. Sakuda and H. Bando, Prog. Theor. Phys. **78** (1987) 1317.

[27] T. Yamada, T. Motoba, K. Ikeda and H. Bando, Prog. Theor. Phys. Suppl. **81** (1985) 104.

[28] M. May and H. Hotchi, private communication (2002).

[29] T. Hasegawa *et al.*, Phys. Rev. **C 53** (1996) 1210.

[30] D.J. Millener, private communications (1999).

[31] D. H. Davis *et al.*, Nuovo Cim. **22** (1961) 275.

[32] E. Hiyama, *et al.*, Phys. Rev. **C 53** (1996) 2075.

[33] E. Hiyama, private communication (2000).

[34] H. Tamura *et al.*, KEK PS proposal E518 (2002).

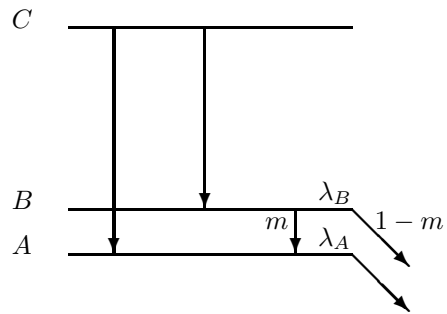[35] H. Bhang *et al.*, Phys. Rev. Lett. **81** (1998) 4321.

Figure 34: Method of $B(M1)$ measurement from coincidence events of γ-ray and weak-decay particles.
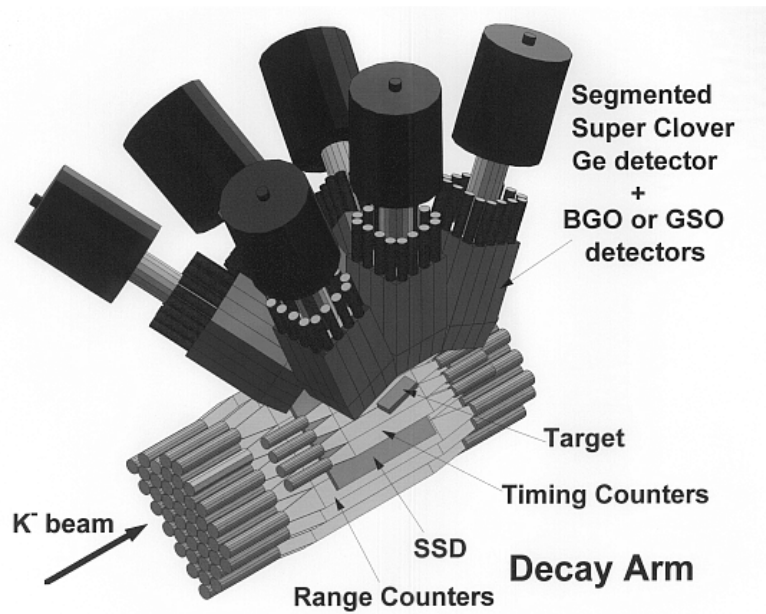

Figure 35: A half side of the setup for the weak-γ coincidence experiments to measure $B(M1)$ or $B(E2)$ using the lifetime measurement with weak-decay particles.
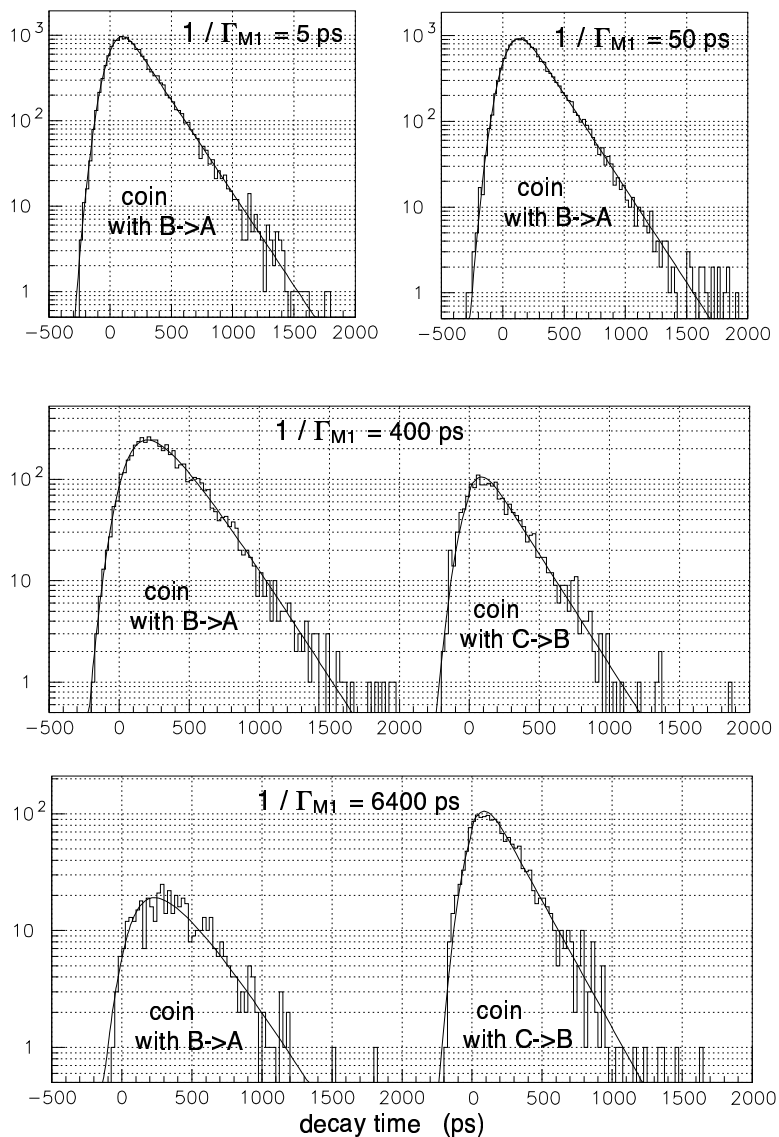
Figure 36: Simulated time spectrum of weak-decay particles of $^{12}_{\Lambda}$C measured in coincidence with B→A (the spin-flip $M1(2^- \to 1^-)$ transition) and with C→B (the $1^-_1 \to 1^-$ transition) for various values of the B→A transition rate (Γ_{M1}). A time resolution of 200 ps FWHM is folded. By fitting these two histograms simultaneously to the expected functions (see text), both decay rates λ_A and λ_B can be determined within 5% statistical errors.
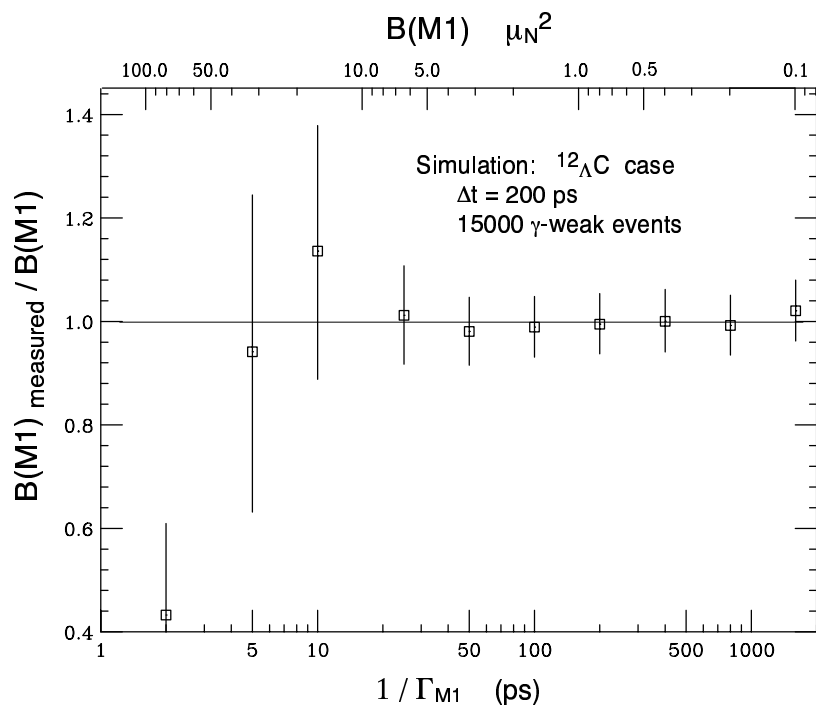
61

Figure 37: Sensitivity of $B(M1)$ measurement for $^{12}_\Lambda$C case. See text for the conditions of the simulation.

A   Future of Hypernuclear Research...........by R.E. Chrien

R.E. Chrien [1],
Brookhaven National Laboratory, USA

A.1   Preface

This document is a statement of interest made on the behalf of scientists at Brokhaven National Laboratory who are supportive of research initatives at the Japanese Hadron Facility. This area of research is important for the ultimate understanding of hadronic forces and it is not being actively pursued elsewhere. The JHF thus serves to bridge a serious gap which has developed in the world-wide advancement in the state of scientific research.

This statement is the personal expression of the views of the author. While I cannot claim to represent the views of other scientists at the Laboratory, I believe them to be generally sympathetic to the views expressed here. I cannot claim to represent the BNL managers, nor the various funding agencies. It must not be construed as offering any commitment of funds, equipment, or resources. Any such commitment will result from official actions to be taken at a future time. However, it is the opinion of the author that such official action is necessary to the health of an important segment of nuclear physics research. Suggestions concerning the use of equipment, scientific efforts, and other resources are made in this pages.

The sections that follow contain the areas recommended by the author and arranged sequentially according to his perceived priorities. As appropriate, suggested resource needs are contained in each section.

A.2   Doubly-Strange Systems

One of the most exciting developments in recent years in the advance in our ability to explore the forces among nucleons and baryons with newly-developed techniques. The knowledge of baryon interaction models has heretofore been hampered by the lack of a reasonable data base in the strangeness sector. The following subsections describe two such techniques which should be actively pursued as soon as practicable. They offer the hope of filling in the gaps in the strangeness "chart of the nuclides".

A.2.1   Study of $\Lambda\Lambda$ Hypernuclei by Sequential Pionic Decays

The (K^-, K^+) reaction can place two units of strangeness in the same target nucleus. The resulting pair of Λ hyperons have a significant chance of interacting. A possible signal of such an interaction is the generation of a sequential pair of pions, each associated with one unit of strangeness change. In the BNL-AGS E906 experiment, evidence was obtained for a substantial production of the nucleus $_{\Lambda\Lambda}^{4}H$ a result, which if confirmed, would largely rule out the existence of an H-dibaryon. The proposed existence of $_{\Lambda\Lambda}^{4}H$, a very loosely-bound system, would make it an ideal test bed for studies of Λ-Λ interactions. A follow-on experiment (AGS-E961), using a lithium target, has been approved by the BNL-AGS PAC, but is scheduling is doubtful because of lack of funding. This experiment is important for

---

[1]Other interested scientists at BNL are the following: P.H. Pile, A. Rusek, M. May, D.J. Millener, and S.H. Kahana.

an understanding of doubly-strange systems in hydrogen and helium hypernuclides, i. e. the s-shell hypernuclides.

A.2.2   Study of ΛΛ Hypernuclei by the hybrid-emulsion technique

The recent publication of the so-called "Nagara" event, produced by the Japanese KEK facility, has suggested that the pairing energy among Λ hyperons is exceedingly weak, of the order of perhaps 1.0 MeV. The development of an efficient and selective hybrid emulsion technique has offered the hope of a comprehensive study of doubly-strange systems which would span the hypernuclear p-shell, and even beyond. An extension of this work has been approved by the BNL-AGS PAC, but as is the case of the sequential decay experiment cited above, is scheduling is doubtful. These two experiments should be done as soon as possible at the new facility.

A.2.3   Ξ Hypernuclei

In spite of the strong decay of the Ξ hyperon in the nuclear medium, it has long been speculated that Ξ excitations might be sufficiently long-lived to be observable. Although such speculations proved to be misleading in the case of the Σ hyperon, there is no decisive experimental evidence in the case of Ξs. Such evidence could be provided at JHF. What is required is a spectrometer with a resolution sufficient to isolate such levels. The existing device at the AGS D6 line, with a resolution of ≈ 16 MeV/c is not adequate.

A.3   Singly-Strange Systems

A.3.1   High Resolution γ-Ray Spectroscopy

The introduction of large acceptance, high resolution, and highly segmented germanium detectors arrays has revolutionized low energy nuclear physics, and promises to do the same for the strangeness sector. Recent experiments have demonstrated the remarkable ability of the Λ hyperon to stimulate a nuclear compression which creates a large alteration in the resulting level schemes. This compression effect is difficult to produce, because of the Pauli Principle, in the non-strange sector. It is easy to see in hypernuclei. High resolution spectroscopy in the p-shell is necessary to compare nuclear level positions against ΛN model predictions, and to deduce the sizeable effective 3-body forces induced by the presence of the Σ hyperon nearby in mass. The (K^-, π^-) reaction with a K^- beam below 1.0 MeV/c, is an ideal way to produce radiative decays because of the small momentum transfer involved. What is needed to advance the technique beyond what has recently been achieved at the BNL-AGS, is a high resolution, high acceptance magnetic spectrometer to isolate the γ-production region by selecting the missing mass in the reaction. A magnet with the capabilities of the old Moby-Dick, or better, is a requirement.

A.3.2   Spectroscopy of Λ Hypernuclei with the (π^+, K^+) reaction

The (π^+, K^+) reaction, first perfected as a spectroscopic tool for studying hypernuclear excitations at the BNL-AGS has been very useful for mapping out energy levels across virtually

the whole periodic table. It has been employed with the SKS superconducting spectrometer over the past decade, and has been especially effective in determining positions of the core-excited states in the hypernuclear p-shell. It would be a useful complement to the γ studies carried out with the 1.1 GeV/c beamline. The SKS, when applied to the (π^-, K^+) reaction in the quasi-free region, has proved useful for studying the Σ well depth. It is natural to employ it for a continuation of these studies at the JHF.

A.3.3 Exploring Mirror Nuclei with the (K^-, π^0) Reaction

To date, almost all hypernuclear counter experiments involve the replacement of a nuclear neutron by a Λ hyperon. It would be informative to supplement that information by producing mirror nuclei to those produced by strangeness excahnge or associated production. This, however, would involve the detection of a π^0, using a device such as a neutral meson spectrometer. A detailed comparison of mirror level schemes would explore the interesting questions about the nuclear role of charge symmetry. A number of attempts were made to use this reaction at the BNL-AGS with the NMS developed at Los Alamos. The limited acceptance of the NMS, however, precludes its use with in-flight kaon reactions, and the use of stopping kaons produces high backgrounds. A program of measurements at the JHF would require an alternative method for neutral meson detection, such as available in a highly-segmented photon detector. Such a device, the Crystal Ball, was used in several experiments at the AGS. This device has a large acceptance, and has been shown to be rather insensitive to neutron backgrounds. If available, this device would be useful in pursuing this topic with in-flight studies at the JHF.

A.3.4 Strangeness-changing Weak Decays

The topic of strangeness-changing weak decays has been the subject of much hypernuclear research over the past 50 years, especially in nuclear emulsion studies. Questions about the weak decay Hamiltonian abound, and focus on the short-range part of the interaction. It has been speculated that weak decay studies might exhibit effects which require the application of QCD to explain. The non-mesonic decays, and especially the neutron-induced decays, have been hard to measure and hard to model with theory. Clearly weak decay experiments should play a role in the JHF program. At the BNL-AGS, the NMS (the Neutral Meson Spectrometer, originally built at Los Alamos), was used with a large neutron detector array, in an attempt to measure the validity of the $\Delta I = 1/2$ rule in hypernuclear decays. As with the remarks above concerning the role of nuclear isospin, the use of NMS was severly limited due to its low acceptance and background sensitivity. An alternative detector, like the Crystal Ball cited above, should be considered.

A.3.5 Hyperon-Nucleon Scattering

There is a real need for scattering data involving hyperons and nucleons for constraining nuclear models within the SU_3 framework. KEK has been the site for a scattering experiment using a scintillation fiber target and image intensifiers. Such an experiment would investigate the $(\Xi p \to \Lambda\Lambda)$ reaction and establish the role of Ξ's in the nuclear medium.

A.3.6 Search for deeply-bound kaonic states

Following the unexpected observation of nuclear pionic states, a natural question arose: are there deeply bound kaonic states which have sufficiently long lives to be observable? Such states arise, for example, when the absorption of low-lying kaon atomic states in the nuclear medium occur. The observation of such states would shed considerable light on the nature of the kaon-nuclear potential well. Although proposed for the BNL-AGS, the lack of accelerator funding for the AGS makes the JHF the only practical alternative for such investigations.

A.4 Instrumentation Remarks

A number of experiments listed above have instrumental requirements which are summarized here. Since there are few, if any, competitive facilities for these presently-existing instruments, it is plausible to argue that their acquisition is possible and the instrumental expenses at the JHF can be significantly reduced.

The first item to be noted concerns beam lines for providing separated kaon beams. It is clear that the best kaon lines existing are at the BNL-AGS in the C2 (1.0 GeV/c) and the D6 (2.0 GeV/c) areas. They offer the world's best purities. Should the AGS lack funding for further fixed-target, slow-extraction running, those lines should be considered for transfer to the JHF. I urge management and the funding agencies to consider such transfers as part of the US involvement in the JHF program.

Secondly, several of the experimental programs above, particularly the spectroscopic studies, require a much better spectrometer than has been used at the AGS-D6 line. Although the acceptance of the 48D48 BNL spectrometer is adequate, its poor resolution makes it unacceptable at JHF. BNL can probably not help in this area. There may be other spectrometers elsewhere, and I urge our colleagues to locate them. One such example of a possible useful–if not vital–instrument, is the Crystal Ball(originally built at SLAC), and now located at Mainz.

Thirdly, a number of BNL staff scientists have been deeply involved in hypernuclear research in several areas: instrumental, experimental, and theoretical. I believe that they wish to remain active in a JHF-US collaboration, and hope that a fruitful relationship can be maintained. I urge BNL management to promote those ties.